Automatic Generation Control Using Particle Swarm Optimization for Enhanced Renewable Energy Integration in Hybrid Systems

Surafel Belayneh Asres

A Thesis Submitted to Department of Electrical Power and Control Engineering

School of Electrical Engineering and Computing

Presented in Partial Fulfillment of the Requirement for the Degree of Master's in Electrical Power and Control Engineering (Specialization in Power Engineering)

Office of Graduate Studies

Adama Science and Technology University

May, 2024

Adama, Ethiopia

Automatic Generation Control Using Particle Swarm Optimization for Enhanced Renewable Energy Integration in Hybrid Systems

Surafel Belayneh Asres

Advisor: Prof. S Kim

A Thesis Submitted to Department of Electrical Power and Control Engineering

School of Electrical Engineering and Computing

Presented in Partial Fulfillment of the Requirement for the Degree of Master's in Electrical Power and Control Engineering (Specialization in Power Engineering)

Office of Graduate Studies

Adama Science and Technology University

May, 2024

Adama, Ethiopia

Declaration

I hereby declare that this Master thesis entitled "Automatic Generation Control Using Particle Swarm Optimization for Enhanced Renewable Energy Integration in Hybrid Systems" is my original work. That is, it has not been submitted for the award of any academic degree, diploma or certificate in any university. All sources of materials that are used for this thesis have been duly acknowledged through citation.

____________________ ____________________ _______________

Name of student	Signature	Date

Recommendation

I, the advisor of this thesis, hereby certify that I have read the revised version of the thesis entitled "Automatic Generation Control Using Particle Swarm Optimization for Enhanced Renewable Energy Integration in Hybrid Systems" prepared under my guidance by Surafel Belayneh Asres submitted in partial fulfillment of the requirements for the degree of Masters of Science in Electrical Power and Control Engineering. Therefore, I recommend the submission of the revised version of the thesis to the department following the applicable procedures.

Major Advisor	Signature	Date

Approval Page of M.Sc. Thesis

I, the advisors of the thesis entitled "Automatic Generation Control Using Particle Swarm Optimization for Enhanced Renewable Energy Integration in Hybrid Systems" and developed by Surafel Belayneh Asres, hereby certify that the recommendation and suggestions made by the board of examiners are appropriately incorporated into the final version of the thesis.

______________________	______________	______________
Major Advisors	Signature	Date

We, the undersigned, members of the Board of Examiners of the thesis by Surafel Belayneh Asres have read and evaluated the thesis entitled "Automatic Generation Control Using Particle Swarm Optimization for Enhanced Renewable Energy Integration in Hybrid Systems" and examined the candidate during open defense. This is, therefore, to certify that the thesis is accepted for partial fulfillment of the requirements for the degree of Master of Science in Electrical Power and Control Engineering.

______________________	______________	______________
Chairperson	Signature	Date
______________________	______________	______________
Internal Examiner	Signature	Date
______________________	______________	______________
External Examiner	Signature	Date

Final approval and acceptance of the thesis is contingent upon submission of its final copy to the Office of Postgraduate Studies (OPGS) through the Department Graduate Council (DGC) and School Graduate Committee (SGC).

______________________	______________	______________
Department Head	Signature	Date
______________________	______________	______________
School Dean	Signature	Date
______________________	______________	______________
Office of Postgraduate Studies, Dean	Signature	Date

ACKNOWLEDGEMENTS

First and foremost, I want to praise the Almighty God, without whom the progress of this thesis would have been impossible. Next, I'd like to express my appreciation to Professor S Kim, for his professional advice, invaluable assistance, guidance, and support. Throughout this thesis, he has been a continual source of inspiration. I'd also want to express my gratitude to the members of the Electrical Power and control Engineering department for their continuous encouragement during the thesis progress. Finally, I'd want to express my gratitude to my family and friends, who have always encouraged me to finish my work.

CONTENTS

List of Figures

List of Tables

Acronyms and Abbreviations

AC	Alternating Current
ACE	Area Control Error
AGC	Automatic Generation Control
BFOA	Bacterial Foraging Optimization Algorithm
BMS	Battery Management system
CAES	Compressed Air Energy Storage
CBES	Chemical Battery Energy Storage
DC	Direct Current
ES	Energy Storage
ESS	Energy Storage System
FESS	Flywheel Energy Storage system
GA	Genetic Algorithm
ITAE	Integral Time Absolute Error
KW	Kilowatt
MW	Megawatt
PI	Proportional Integral
PID	Proportional Integral Derivative
PSO	Particle Swarm Optimization
PV	Photovoltaic
RES	Renewable Energy Source
SCES	Supercapacitor Energy Storage
SMES	Superconducting Magnetic Energy Storage
VRFB	Vanadium Redox Flow Battery
WT	Wind Turbine

Abstract

In recent years, there has been a significant increase in the penetration of renewable energy sources in to the power systems around the world, due to the need for sustainable energy sources and the reduction of greenhouse gas emissions. The integration of multiple renewable energy sources can enhance the reliability and efficiency of renewable energy systems. However, the integration of multiple renewable energy sources requires efficient control strategies to optimize their performance and ensure reliable operation because of the uncertainties and intermittent of RES. Automatic generation control plays a vital role in controlling the integration of hybrid systems by ensuring adjustments to power generation, optimizing energy storage and maintaining power system stability between different control areas. Most of the time the interconnected power systems in the AGC relies only on the synchronous generating units because of the challenges due to intermittent and variable nature of renewable energy sources. This thesis proposes AGC for integrating hybrid system incorporating with renewable energy sources (PV and wind) and energy storage system (VRFB and FESS) to overcome those challenges. A two-area AGC system model was developed to regulate frequency and system stability by adjusting generation based on load deviations. PID controller was used as a control strategy for the proposed system. This PID controller was optimized through an effective Particle Swarm Optimization technique. The objective of applying PSO algorithm was to tune PID controller in order to get optimal parameters of the controller gains. Then the power system achieved a significantly improved settling time, maintained grid frequency within the specified limits and mitigated variations in tie line power between the control area. The simulation results confirm the effectiveness of the proposed automatic generation control using particle swarm optimization for enhancing renewable energy integration in hybrid systems. This was achieved through significantly improved settling time, better grid frequency regulation and reduced tie-line power deviations. This study offers a promising solution for addressing the challenges associated with renewable energy integration.

***Key word**: Automatic Generation Control, Particle Swarm Optimization, Vanadium redox flow battery, flywheel energy storage*

CHAPTER ONE

INTRODUCTION

1.1 Background of the Study

Moving towards a clean and low-carbon energy future depends on incorporating renewable energy sources like solar, wind, hydro, geothermal, and biomass into power grids. These renewables offer a plentiful, clean, and constantly refillable alternative to traditional energy sources. They are key to cutting greenhouse gases, fighting climate change, and making our energy supplies more secure (Martins, 2023). However, because these sources can be unpredictable and inconsistent, managing a stable and reliable power grid becomes more complex. Therefore, integrating renewables effectively requires finding creative solutions to overcome these challenges and enable the effective integration of variable renewable energy generations.

Power systems are divided into control areas linked by tie lines for exchanging power. Each area's capacity is determined by the generators within it. Automatic generation control (AGC) is crucial for maintaining consistent grid frequency and power flow across tie lines during normal operation and minor load changes. In recent decades, there's been a surge in research on AGC, aiming to improve power grid operation, control, and stability. Various control strategies have been implemented, including artificial neural networks, fuzzy logic, and robust controllers (Panda et al., 2013). However, these methods struggle with changes in system parameters and nonlinearities. Designing optimal controllers for AGC remains a significant challenge. To address this, researchers have employed various optimization techniques like genetic algorithms, particle swarm optimization, teaching learning-based optimization and so on to design these controllers effectively within interconnected power systems. For realistic studies that consider uncertainties, incorporating different types of renewable energy sources (RES) into the AGC model is essential (Hasanien, 2017).

The recent years have seen a surge in renewable energy sources (RES) being integrated into power grids. According to the Global Wind Energy Council, wind power installations reached a record high of 117 gigawatts (GW) in 2023, a whopping 50% increase compared to the previous year. This brings the global total wind power capacity to an impressive 906 GW by the end of 2023 (GWEC, 2023). Solar power is keeping pace as well, statistics from the world

PV market show a near 50% increase in total installations, reaching nearly 510 GW in 2023, which is the fastest growth rate in the past two decades (Dr. Ajay Mathur, 2023). These statistics indicate the high level of penetration of the RES into the electric power grids. Not only RES but also the energy storage systems integrated to the power systems to storing excess energy during times of high generation and releasing it when needed. Energy storage technologies help to balance supply and demand, smooth out fluctuations RES output, improve stability and frequency regulation. Building on the idea of including different RES types in the AGC model, this highlights another challenge for control system designers: dealing with the intermittent and unpredictable nature of renewable energy sources. Fortunately, advancements in computational evolutionary algorithms offer a promising solution to fine-tuning controller parameters within the AGC loops, potentially helping to overcome these challenges.

Particle Swarm Optimization (PSO) is a widely used optimization technique which is inspired by the flocking behavior of birds. This algorithm iteratively improves a set of candidate solutions called particles, by leveraging their individual experiences and the collective knowledge of the swarm. It was introduced by Kennedy and Eberhart in 1995 (Shaikh & Yadav, 2022). PSO stands out due to its fast convergence speed and minimal parameter tuning requirements. This makes it particularly attractive for complex optimization tasks. The algorithm's recent success in solving diverse mathematical and engineering problems highlights its potential for Automatic Generation Control (AGC) in interconnected power systems (Li et al., 2021).

This thesis explored the use of Particle Swarm Optimization (PSO) to fine-tune PID controllers within an Automatic Generation Control (AGC) system for interconnected power systems. This system incorporates renewable energy sources (RES) like wind and solar power, along with energy storage solutions like vanadium redox flow batteries and flywheel storage. Realistic data for wind speed, solar irradiation, and temperature is used to model these RES and Energy Storage System (ESS) components within the AGC framework. This allows for a more accurate study of AGC challenges in a real-world interconnected power system. To optimize controller performance, the thesis employs the integral time absolute error (ITAE) criterion, a common metric in AGC analysis. The effectiveness of the PSO-based PID controller is then evaluated by comparing its performance against a standard, non-optimized

PID controller in a multi-area power system under various operating conditions. Finally, simulations conducted using MATLAB software validate the proposed control strategy's efficacy in managing the complexities of an AGC system with integrated RES and ESS components.

1.2 Statement of the problem

The integration of renewable energy sources into power systems has accelerated in recent years. This surge is driven by growing concerns about climate change, energy security, and the dwindling reserves of fossil fuels. However, this integration has several challenges. The variability and intermittency of renewable energy sources can pose significant challenges for the stability and reliability of the power system. Renewable energy sources are dependent on weather conditions and can experience fluctuations in generation. This variability can create imbalances between supply and demand leading to power system instability and reliability issues. This integration of renewable energy sources and energy storage require a control system that can effectively manage the fluctuations in power generation and demand. Unless otherwise the system may experience instability due to fluctuations in power generation, the frequency may deviate and affecting the overall stability and performance of the hybrid system. In the absence of effective control system, the charging and discharging of this storage system may not be optimized and also affecting their overall efficiency and lifespan.

1.3 Objectives

1.3.1 General Objective

The general objective of this thesis is to develop and implement an Automatic Generation Control (AGC) using Particle Swarm Optimization (PSO) to enhance the integration and performance of hybrid renewable energy systems.

1.3.2 Specific Objective

- ✓ To model two area AGC system.
- ✓ To model PV/wind/VRFB and FESS and integrate to the AGC system.
- ✓ To develop PSO based optimization algorithm for tuning the PID controller parameters within the AGC system.
- ✓ To achieve effective frequency and tie line power regulation.
- ✓ To ensure the stability of power system during integration of renewable energy.

1.4 Limitations of the Thesis

This thesis has some limitations in a few areas. The model relies on two area automatic generation control system integrated with hybrid renewable energy system and energy storage system. The output power is used in case of renewable energy sources and for the energy storage system output power and other specifications of the storage system was used. The hybrid system consists of PV and wind power generation from renewable energy sources. VRFB energy storage system and flywheel energy storage system from energy storage systems. Additionally, the thesis relies on simplified power system model for efficient simulation purposes.

1.5 Expected Outcomes of the Thesis

The expected outcomes of this thesis would likely be demonstrating the effectiveness of using particle swarm optimization for automatic generation control in hybrid power systems that integrate renewable energy sources. Improving the reduction in frequency deviations and tie line power deviations experienced by the system after implementing PSO based AGC. Finally comparing the performance of PSO based AGC against conventional methods in terms of frequency and tie line power regulation metrics.

1.6 Significance of the Thesis

This thesis holds significant value for the advancement of a sustainable and reliable energy future. By focusing on integrating renewable energy sources with energy storage systems, it proposes a solution to mitigate the intermittency of renewables and create a more stable and reliable power system. This shift from fossil fuels to clean energy sources not only reduces our environmental footprint but also offers a potential pathway to combat climate change. Furthermore, the research contributes to the ongoing development of renewable energy and energy storage technologies, paving the way for practical applications in real-world energy systems. Finally, it has better performance on regulating the change in frequency and tie line power occurred because of the integration of renewable energy and energy storage system into power systems.

CHAPTER TWO

LITERATURE REVIEW

2.1 Introduction

The urgent need for sustainable energy solutions has driven the rapid integration of renewable sources like solar and wind power into our power systems. However, these resources are intermittent, making it difficult to maintain grid stability and frequency control. To address this issue, researchers have proposed different integration system with various control strategies and optimization techniques. This literature review aims to provide an overview of the research findings related to the particle swarm optimization based automatic generation control incorporating with hybrid PV/Wind/Vanadium Redox Flow Battery/Flywheel system for enhancing renewable energy integration. Several studies have investigated on the integration of hybrid PV, wind, vanadium redox flow battery, and flywheel systems into AGC frameworks.

2.2 Hybrid PV/Wind/VRFB /FESS

Hybrid renewable energy systems combining with energy storage are gaining traction due to their ability to address the intermittency challenges of renewable energy sources. A literature review on this topic would explore the recent advancements in integrating RES and ESS in to power systems. So, let us see some the literature.

Castillo and Gayme (Castillo & Gayme, 2014) studied grid-scale energy storage applications in renewable energy integration. The study emphasized the role of energy storage systems, such as vanadium redox flow batteries and flywheels, in mitigating the challenges associated with the integration of renewable energy into the grid. The findings highlighted the potential of energy storage technologies to enhance grid stability, manage fluctuations in renewable energy generation, and support the reliable integration of multiple renewable energy sources. But this thesis not used AGC as a controlling part the system is not automatic.

Palanisamy and Padmanaban, (Palanisamy & Padmanaban, 2018) presented an intelligence-based battery management system (BMS) for an optimized dual-VRB in a wind-PV hybrid system. The research findings highlight the implementation of VRB in a hybrid system, but do not specifically discuss the integration of flywheel systems or their role in AGC.

Merei et al (Merei et al., 2014) conducted an optimization study of an off-grid hybrid power supply system based on battery aging models for different battery technologies. While the research provides insights into battery optimization, it does not specifically address the integration of hybrid PV, wind, VRB, and flywheel systems in AGC.

Dassisti et al (Dassisti et al., 2021) reviewed on storage systems in the scenario of penetration of renewable energy sources. Mainly they focus on vanadium redox-flow batteries in combination with a wide range of renewable energy sources. They proposed Vanadium Redox Flow Batteries (VRFBs) as a particularly attractive electrochemical storage technology due to their unique advantages. VRFBs offer independent scaling of energy capacity and power output, fast response to fluctuations, room temperature operation for simplified maintenance, exceptionally long lifespans, and minimal environmental impact. The study also explores VRFB applications and compares them to other storage systems, with a detailed table as shown in table 2.1. As shown in the table below vanadium redox flow have better performance

Table 2.1 Comparison between VRFB and other conventional batteries (Dassisti et al., 2021)

Parameters	VRFB	Lithium	Lead acid
Service life	15-20 years	3-5 years	2 years
Depth of discharge	100% (> 10,000 cycles)	80% (2500 cycles)	50% (700 cycles)
Energy Den.	18-45 per Wh	300-400 per Wh	60 per Wh
Cost	200-400 ₤ per kWh	120-300 ₤ per kWh	600-100 ₤ per kWh
Operational risks	Safe	Not safe	Not safe
Life cycle assessment	Have very low environmental impact, because vanadium electrolyte is 100% recyclable	Low environmental impact	have environmental impact because of lead, which is a heavy and toxic metal

When compared with the lithium and lead acid battery because of this VRFB are selected in this thesis as energy storage system.

Martínez et al (Martínez et al., 2017) proposed an optimal sizing method for VRB to provide load frequency control in power systems with intermittent renewable generation. Although the study focuses on VRB sizing, but the work does not address the integration of hybrid PV, wind, VRB, and flywheel systems in AGC.

Suvire et al (Suvire et al., 2017) investigated the combined control of a flywheel energy storage system and a VRB for wind energy applications in microgrids. The research findings shed light on the integration of flywheel and VRB systems in AGC, specifically in the context of microgrids. However, the study does not specifically address the incorporation of hybrid PV, VRB, and flywheel systems in AGC.

Kai Xu et al (Xu et al., 2023) investigated how flywheel energy storage systems (FESS) can improve the stability and quality of power grids. They proposed that FESS offers several advantages over other storage technologies, including a long lifespan, high efficiency, high power density, and minimal environmental impact. The study also explored the key components of FESS, such as flywheel rotors, motors, bearings, and power electronics. As shown in detailed in table 2.2 they compare FESS with another storage system. As shown in table below SCES and FESS have better performance than another energy storage technologies because of their charging time, operating temperatures, response time, life span and their environmental features. Since SCESs are highly affected by environmental requirements like temperature and humidity, FESS are selected in this thesis to integrated to the power system.

Table 2.2 Comparison of energy storage systems (Xu et al., 2023)

Features	CAES	CBES	SMES	SCES	FESS
Efficiency (%)	40-60	70-80	80-95	80-95	85-95
Specific energy (Wh/kg)	-	3-15	1-10	0.2-10	5-150
Specific power (W/kg)	-	100-700	1000	7000-18,000	180-1800
Charging time	Hr	Hr	Hr	Min	Min
Discharge time	1-20h	1min-hour	10ms-15min	0.1s-1 min	15s-15min
Response time	Min	Millisecond	Millisecond	Millisecond	Millisecond
Service life	> 20	3-15	> 20	> 20	> 20
Maintenance cycles	frequent	< 6months	frequent	> 10 years	> 10 years
Operating temperatures	35 to 50	-10 to +300	4.2 to 77 K	-30 to +50	-40 to +50
Environment requirement	high	medium	very high	high	low
Environmental features	Non pollutant	Pollutant	Non pollutant	Non pollutant	Non pollutant

2.3 PSO and AGC System

One of the key challenges in the integration of RES is the intermittency and variable variations of the renewable energy which causes to the power system instability and unreliable. Automatic generation control has potential to controlling and improving the challenges by using different optimization technique like particle swarm optimization (PSO), genetic algorithm (GA), whale optimization algorithm (WOA) and so on. This literature review aims to analyze the research findings on particle warm optimization and AGC system.

Hany M Hasanien (Hasanien, 2017) proposed a new power system model incorporating both conventional and renewable energy sources to analyze the Automatic Generation Control (AGC) problem. This model utilizes a PID controller optimized by the whale optimization algorithm (WOA) for control strategy within the AGC loops. It's important to note that energy storage systems were not included in this particular study.

Ghoshal (Ghoshal, 2004) explores novel optimization techniques for PID gains within a fuzzy logic based Automatic Generation Control (AGC) system. The paper proposes three methods: particle swarm optimization (PSO), hybrid PSO, and hybrid genetic algorithm (GA). Their study reveals that PSO achieves superior optimization of PID gains compared to GA and hybrid GA. It's important to note that this research focused solely on optimization techniques and did not explore the integration of hybrid renewable energy sources (RES) or energy storage systems (ESS) into the AGC system.

Tasnin and Saikia (Tasnin & Saikia, 2018) compared the performance of various energy storage devices (battery, flywheel, capacitive, superconducting magnetic, ultra-capacitors, and redox flow) for automatic generation control (AGC) in a complex power system. This system incorporated thermal, hydro and a geothermal power plant. Their analysis, under a specific controller design, revealed that vanadium redox flow batteries (VRFB) outperformed all other storage options in terms of AGC performance.

Kumar and Shankar (Kumar & Shankar, 2021) proposed a method for integrating Automatic Generation Control (AGC) into a two-area deregulated power system, even though the specific details of renewable energy source integration aren't explicitly addressed. Their approach utilizes a PID controller optimized by a new quasi opposition lion optimization algorithm to achieve the desired dynamic response. Additionally, to dampen AGC system oscillations, they explore a hybrid energy storage system combining redox flow batteries and superconducting magnetic energy storage.

Panda et al. (Panda et al., 2013) introduced a hybrid BFOA-PSO algorithm for AGC of linear and nonlinear interconnected power systems. The paper used PI controller and demonstrated that the proposed approach achieved superior performance compared to other optimization algorithms. The hybrid algorithm effectively optimized the AGC system, ensuring stability and reliability. But the study doesn't include the renewable energy sources and storage systems.

Gozde and Taplamacioglu (Gozde & Taplamacioglu, 2011) presented a novel approach to Automatic Generation Control (AGC) in thermal power systems using a craziness-based Particle Swarm Optimization (PSO) algorithm. Their method employs a PI control strategy for a two-area thermal system, demonstrating significant optimization of the AGC performance. The results highlight improved dynamic response through the optimized PI controller, leading to enhanced overall system stability. This paper emphasizes the effectiveness of PSO algorithms in achieving optimal controller design for AGC applications in thermal power systems and did not explore the integration of renewable energy sources or energy storage systems.

As those literatures shows PSO optimization was excellent choice for the interconnected power system by using AGC. Because of the its several advantages like faster convergence, fewer calculations, ease for implementation and robustness. Therefore, PSO was used in this thesis as an optimization technique to get the optimal values of the controllers.

2.4 Hybrid Renewable Energy Sources

2.4.1 Flywheel Energy Storage System

Integrating an Energy Storage System (ESS) to solar and wind farms helps smooth out the natural ups and downs of these renewable energy sources. Flywheel Energy Storage Systems (FESS) are a great option for this purpose. They work by storing energy as the spinning motion (kinetic energy) of a flywheel, which can then be converted back to electricity when needed (Qin et al., 2023). FESS boasts several advantages like they can pack a lot of power into a small space (high power density), function well in various environments (insensitivity to environmental conditions) and avoid the use of harmful chemicals.

Working Principles and components of FESS

Flywheel Energy Storage Systems (FESS) operate like a spinning reservoir of energy. A high-speed motor whirs a heavy flywheel made of steel or composites, storing incoming electricity as kinetic energy – the energy of motion. The faster the flywheel spins, the more energy it holds. When electricity is needed, the flywheel doesn't just coast – it acts like a generator in reverse. As it slows down, the motor captures this rotational energy and converts it back into electricity that feeds back into the grid (Amiryar & Pullen, 2020). To minimize energy loss from air resistance, most FESS operate in a near-vacuum, allowing the flywheel to spin freely. This system excels at delivering bursts of power quickly and can rapidly switch between charging and discharging, making it ideal for responding to fluctuating energy demands. However, FESS typically have a lower overall energy storage capacity compared to batteries and experience some energy loss over time due to friction, even in a vacuum.

In this thesis a flywheel energy storage system was selected among the various energy storage devices available in the market like supercapacitor, battery, superconductor magnetic energy storage system. The reason was because BESS (battery energy storage system) has a higher self-discharge rate over time leading to gradual energy loss when not in use but flywheel systems can maintain their charge for longer periods without significant losses. Additionally, batteries may have a limited number of charge-discharge cycles impacting their overall lifespan, whereas flywheels can often withstand a higher number of cycles. SMES device need extremely low temperatures to maintain superconductivity and often require cryogenic conditions which can be challenging and expensive to maintain whereas flywheel systems operate at ambient temperature. SCESS have lower energy density so they store less energy per unit of volume when compared to flywheel systems and FESS have low environmental impacts (Abazari & Monsef, 2019). Hence considering all those factors, flywheel systems was selected in this thesis.

The flywheel energy storage system usually consists of several key components:

- ✓ A flywheel rotor for energy storage.
- ✓ A bearing system supporting the flywheel rotor.
- ✓ Motor
- ✓ Vacuum chamber
- ✓ Vacuum extraction device

- ✓ A power converter system for charge–discharge conversion, including motors and power electronic devices.
- ✓ Cooling system, as shown in figure below.

As illustrated in figure 2.1, the flywheel rotor is the heart of the Flywheel Energy Storage System (FESS). This rotor, typically constructed from metal or composite materials, spins to store energy. The system leverages this rotation for the bi-directional conversion of electrical and kinetic energy. The permanent magnet synchronous motor plays a key role. During periods of excess power, it acts as a motor, efficiently converting electrical energy into the mechanical energy of the spinning flywheel rotor. This essentially stores energy for later use. When the need arises to fill gaps in power demand, the motor switches roles and acts as a generator. By doing so, it converts the flywheel's stored mechanical energy back into electrical energy that can be fed back into the power system.

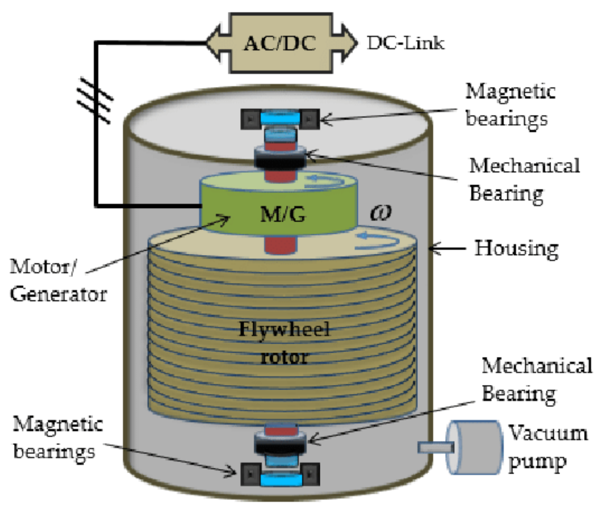

Figure 2.1 Flywheel and its components (Amiryar & Pullen, 2020)

2.4.2 Vanadium Redox Flow battery

Redox Flow Batteries (RFBs) are a rechargeable battery that store energy for power companies. They use chemical reactions to store electricity and release it back when needed. They can store electrical energy by converting to a chemical form through a process called reduction oxidation (redox). This reaction happens within a reactor containing two compartments separated by a membrane. Each compartment holds a unique solution, one with vanadium pentoxide and the other a sulfuric acid solution, and pumps circulate these large volumes of liquids to facilitate the energy storage and release process. A separate diagram illustrates the complete RFB system setup as shown in figure 2.2.

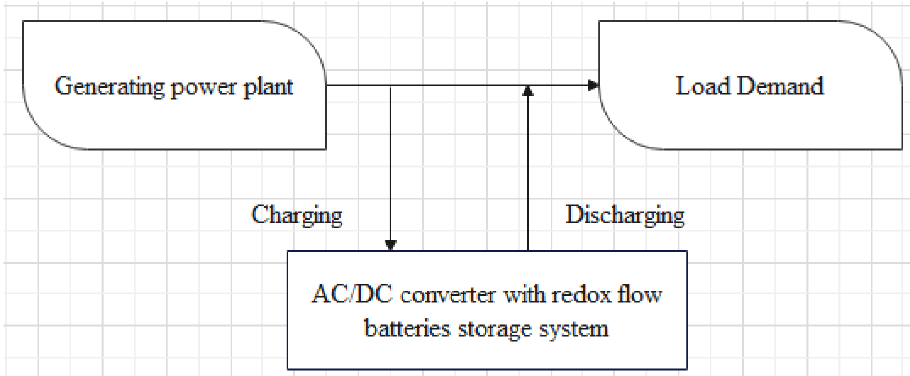

Figure 2.2 General block diagram of VRFB

Redox flow batteries (RFBs) address the challenge of unequal electricity supply and demand by acting as giant storage buffers. They cleverly utilize periods of low demand to charge by converting electricity into chemical energy. When surges or peak loads hit the system, RFBs can instantly release this stored energy back into the grid. A special converter handles any necessary AC/DC conversions to seamlessly integrate with the grid. This ability to bridge the gap between generation and consumption makes RFBs ideal for Automatic Generation Control (AGC) in interconnected power systems. It's important to note that while highly effective, RFB models can be complex due to their non-linear behavior.

Working Principles of VRFB

A VRFB system typically consists of three key parts as shown in figure 2.3. Those are tanks to store the vanadium solutions (electrolytes), a special stack that converts chemical energy to electricity (electrochemical stack), and a pump system that circulates the electrolytes between these components.

Vanadium redox flow batteries (VRBs) function through a unique interplay between chemistry and fluid movement. The key player is vanadium, a metal existing in four different oxidation states within a sulfuric acid solution. These varying states essentially represent different electrical charges vanadium can hold. During charging, electricity flows through the battery, prompting vanadium ions on one side (positive) to lose electrons and vanadium ions on the other side (negative) to gain electrons. This electron transfer essentially stores energy within the vanadium ions themselves (Puleston et al., 2022).

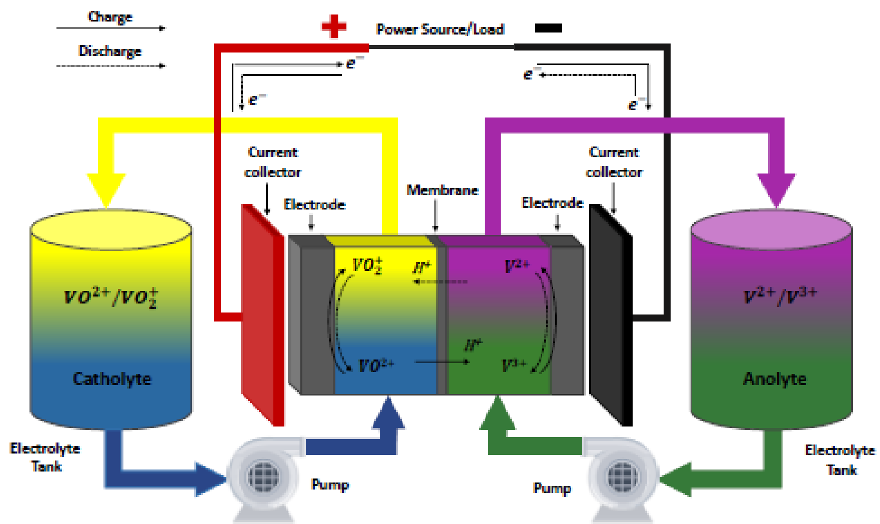

Figure 2.3 General scheme of a VRFB and its main reactions (Puleston et al., 2022)

Sulfuric acid plays a crucial supporting role in this process. It dissolves the vanadium compounds, allowing them to move freely within the solution, and conducts electricity through the movement of tiny charged particles called protons. These protons help maintain electrical balance within the battery. The VRFB itself is like a divided container with a special membrane separating the two halves. Each side holds a unique vanadium solution, and pumps circulate these solutions past the membrane when needed. This circulation, along with the reversal of electron flow between vanadium ions, generates electricity during discharge. The protons from the sulfuric acid solution then flow through the membrane, completing the electrical circuit and delivering power (Lourenssen et al., 2019). This design allows VRBs to boast a key advantage, their energy storage capacity is independent of the internal battery components and instead scales with the size of the external vanadium tanks. This makes VRBs highly suitable for large-scale energy storage applications.

2.5 Summary and Research Gaps

Previous literatures shown that automatic generation control plays a crucial role in maintaining the balance between generation and consumption in power systems with and without penetration of renewable energy sources. PSO was a metaheuristic optimization technique inspired by the social behavior of birds flocking which has been successfully applied in various optimization problems. Despite the effectiveness of in optimization problems, there is a research gap in its application specifically for AGC in hybrid power systems with renewable energy sources. The above literature lacks comprehensive studies on the use of PSO for enhancing the integration of renewable energy sources in AGC systems. This research gap presented an opportunity to investigate the potential benefits of using PSO in AGC for improved stability and efficiency of hybrid power systems with renewable energy sources.

Generally, based on the reviewed literatures, there is limited research focuses on the integration of hybrid PV/wind and integration of energy storage systems in to power system by using automatic generation control. This thesis focused on the integration of those systems into power system by using AGC and optimizing the control strategies for these systems to enhance the overall performance of AGC. In this thesis the advantages and performances of the VRFB and FESS are investigated in order to protect the stability and reliability of power system during the power generation intermittent and variability associated with renewable energy sources and power disturbance occurred in power system. In generals, some data which is used by those literatures are assumed and used in this thesis. For the simulation part, the value of turbine gain, turbine time constant, governor gain, governor time constant, time constant used in the renewable energy and storage systems are extracted from those literatures. There are some limitations on those constants because they aren't standardized which mean differ from one to another literatures. Finally, this thesis evaluating the dynamic response of frequency regulation and reliability aspects of AGC incorporating with hybrid systems by using the optimization techniques.

CHAPTER THREE

MATERIALS AND METHODS

3.1 Materials

In this chapter, mathematical modelling of the components of the automatic generation control is discussed. This automatic generation control system generally consists of six main components: reheat thermal generating units, PV, wind, VRFB, flywheel and particle swarm optimization algorithm. All these components are presented together with their mathematical models in detail.

3.1.2 Software Tools

Simulation will be carried out by using MATLAB/SIMULINK to model the automatic generation control, to design particle swarm optimization technique, to design AGC for PV, to design AGC for wind, to design AGC for VRFB, to design AGC for flywheel and finally all the simulation result will be viewed then from this simulation result, evaluation and comparisons of the results of PSO based AGC for the given hybrid system with normal AGC and with the given hybrid system based on this concept we will try to determine which one is more enhanced for control of renewable energy integration.

The other software used is EdrawMax for creating block diagrams for controlling system of renewable energy integration also for making block diagrams for AGC with PV/Wind/VRFB/ flywheel and make block diagram and flow charts for PSO based AGC for hybrid renewable energy integration. Finally, Microsoft Word is used for writing all data, images and block diagrams in best understandable way and Mendeley was used for the citation and references.

3.2 Methods

In order to achieve the objective of this thesis the system can be approached through several methods. First of all, two area AGC system for the interconnected power system by including the RES and ESS were modelled. After that PID controllers was designed in the AGC loops, then the controller was optimized by using PSO algorithm. The effectiveness of the proposed controller can deal with the RES uncertainties and variabilities. Hence, the result of the simulation can be compared with the non-algorithm controllers and also without/with RES and ESS in the AGC system. As we know the components of the two area AGC system consists of RES (wind and PV) and ESS (VRFB and FESS). For achieving a realistic data, real wind speed data are extracted from Adama I wind power plant are used. Moreover, solar irradiation and temperature data are extracted from a Metehara Solar PV Park project. In addition, the data of storage systems gained from global energy storage database was used. To evaluate the proposed PSO-optimized PID controller's effectiveness, the multi-area power system was simulated under various operating conditions using MATLAB/SIMULINK. The integral time absolute error criterion formed the basis for the optimization problem, ensuring a robust controller for the AGC study.

3.2.1 Integration of Hybrid PV/Wind/VRFB/Flywheel

The integration of a hybrid system combining PV, wind, vanadium redox flow batteries, and flywheels represents a sophisticated and comprehensive approach to renewable energy generation and storage. This hybrid system leverages the complementary strengths of each technology to optimize energy production, storage, utilization and creating a more resilient and sustainable energy infrastructure.

PV and wind turbines harness the abundant and renewable energy from the sun and wind to generate electricity. Solar panels convert sunlight into electricity, while wind turbines capture the kinetic energy of the wind to produce power. By combining these two sources of renewable energy, the hybrid system can maximize energy production and take advantage of the natural variability in solar and wind resources to ensure a more consistent and reliable energy supply.

To address the intermittent nature of solar and wind power generation, the hybrid system incorporates energy storage technologies such as VRFBs and flywheels. VRFBs provide a scalable and long-lasting storage solution that can store excess energy produced during peak generation periods and release it when needed to meet demand. The high cycle life and safety features of VRFBs make them an ideal choice for storing large amounts of energy over extended periods, helping to balance supply and demand in the power system.

In addition to VRFBs, flywheels play a crucial role in the hybrid system by providing fast-response energy storage for short-duration fluctuations in power output. Flywheels store kinetic energy in a rotating mass and can quickly discharge or absorb energy to stabilize grid frequency and voltage. Their rapid response time and high efficiency make flywheels well-suited for providing grid support services such as frequency regulation and voltage control, enhancing the overall reliability and stability of the hybrid system.

This integration in a hybrid system offers multiple benefits beyond individual technologies. By combining renewable energy sources with advanced energy storage technologies, the hybrid system can increase energy self-sufficiency, reduce reliance on fossil fuels, and lower greenhouse gas emissions.

The flexibility and scalability of the system allow for optimal utilization of renewable resources and efficient management of energy flows, contributing to a more sustainable and resilient energy infrastructure. Generally, this integration system represents a forward-thinking approach to renewable energy generation and storage. By harnessing the strengths of multiple technologies in a coordinated manner, this hybrid system can overcome the challenges associated with intermittent renewable energy sources and help accelerate the transition to a cleaner, more sustainable energy future. As the demand for clean energy solutions continues to grow, the integration of hybrid systems like this one will play a vital role in shaping a more resilient and efficient energy system for generations to come.

3.2.2 Working Principle of Hybrid PV/Wind/VRFB/Flywheel

A hybrid renewable energy system that combines PV, wind, vanadium redox flow battery, and flywheel energy storage offers a comprehensive solution for integrating renewable energy sources. The system integrates several components that work together to capture, store, and deliver renewable energy as shown in figure 3.1. Solar PV panels and wind turbines capture sunlight and wind energy, respectively, converting them into electricity. However, these sources are variable, and their output fluctuates depending on weather conditions.

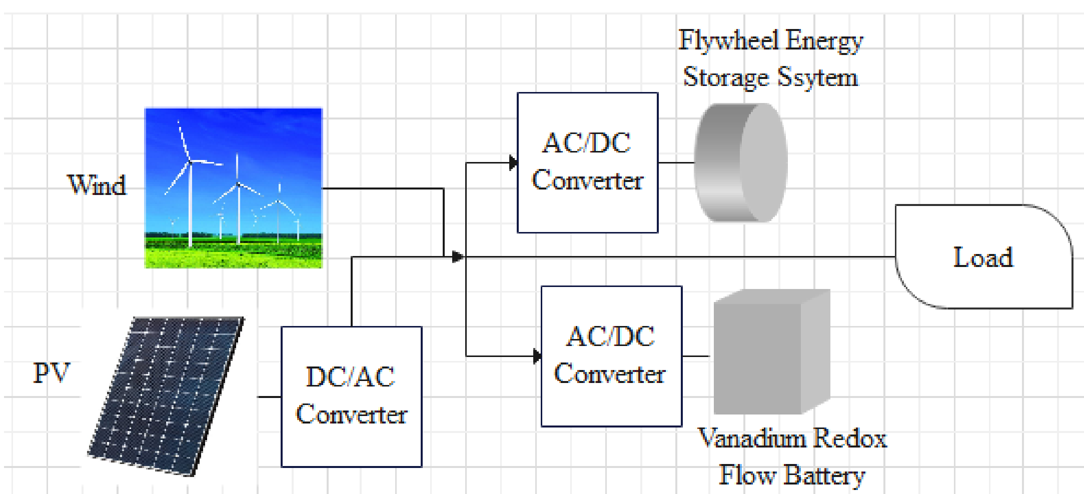

Figure 3.1 Block diagram of the hybrid system

To address this variability, the system incorporates vanadium redox flow battery (VRB) storage. During periods of excess renewable energy generation, the VRB stores electrical energy by changing the valence state of vanadium ions in an electrolyte solution. This stored chemical potential energy can then be converted back into electricity when needed. VRBs are well-suited for managing the inherent variability of solar and wind power due to their ability to store energy for long durations.

The system also incorporates flywheel energy storage. Flywheels store kinetic energy in a rotating mass. When excess renewable energy is available, the flywheel spins up, storing energy. When needed, the flywheel slows down, releasing the stored energy back into the system. Flywheels excel at providing short, high-power bursts, making them ideal for smoothing out rapid fluctuations in renewable energy output.

To ensure efficient operation, a power conditioning system regulates the incoming direct current (DC) output from the PV system and converts the alternating current (AC) output from the wind turbine to DC for compatibility with the VRB. An intelligent management system plays a crucial role in optimizing the charging and discharging cycles for each storage system. It considers factors like renewable energy availability, grid demand, and storage capacity to ensure the system functions efficiently and reliably. By combining these technologies, the hybrid system effectively addresses the intermittency of solar and wind power, offering a reliable, efficient and sustainable solution for renewable energy integration.

3.3 System Modelling

System modelling involves identifying the components used in the proposed system, their interaction and the relations between the components and then using mathematical, graphical and computational tools to describe and simulate the proposed system dynamics. So, under this topic each component of the proposed system was modelled one by one in order to simulate the system and finally see results of the proposed system.

3.3.1 Modelling of Automatic Generation control

The first step in analyzing and designing control systems is creating a mathematical model. There are two commonly used techniques those are the state variable approach and the transfer function method. The state variable method offers the flexibility to handle both linear and nonlinear systems. In contrast, the transfer function method and linear state equations require a system to be linearized first. This linearization process involves making suitable assumptions and approximations to convert the complex system's governing equations into a simpler, linearized form. This thesis will utilize the transfer function method to model the various components within the AGC system.

Generator Load Model

The power loads of AGC composed of loads which remain constant at the rotor speed is changing and a load that change with load frequency or speed changes. Therefore, load change was composed of frequency independent and frequency dependent load types. The frequency dependent load types are very sensitive for small frequency deviations. When the power input increase into the generator load system which is $\Delta P_G - \Delta P_D$, where $\Delta P_G = \Delta P_T$ which is incremental turbine power output by assuming generator incremental loss to be negligible and ΔP_D is the load increment. This increment in power input to the system was described. First, rate of increase of stored kinetic energy in the generator rotor at scheduled frequency (f_0), the stored energy is:

$$W_{KE}^{0} = HP_r \ldots\ldots\ldots\ldots\ldots\ldots\ldots\ldots\ldots\ldots\ldots \text{(3.1)}$$

Where P_r is the KW rating of the turbo generator and H is inertia constant. The second way is when the kinetic energy is proportional to square of speed or frequency, the kinetic energy at a frequency of ($f_0 + \Delta f$) is given by:

$$\frac{W_{KE}}{W_{KE}^{0}} = (\frac{f_0 + \Delta f}{f_0})^2$$

$$W_{KE} = HP_r(\frac{f_0 + \Delta f}{f_0})^2$$

$$W_{KE} = HP_r(1 + \frac{2\Delta f}{f_0} + (\frac{2\Delta f}{f_0})^2)$$

$$W_{KE} = HP_r(1 + \frac{2\Delta f}{f_0})$$

Differentiate both sides, $\frac{dW_{KE}}{dt} = \frac{2HP_r}{f^0}\frac{d}{dt}(\Delta f)$

assume that the change occurred in motor load is sensitive to speed or frequency variation for small change in the system frequency Δf. The rate of change of load with respect to frequency ($\frac{\partial P_D}{\partial f}$) can be regarded as constant for small changes in frequency and can be expressed as:

$$\left(\frac{\partial P_D}{\partial f}\right)\Delta f = \beta \Delta f$$

Where β is frequency bias factor, $\beta = \frac{\partial P_D}{\partial f}$

$$\Delta P_G - \Delta P_D = \frac{2HP_r}{f^0}\frac{d}{dt}(\Delta f) + \beta\Delta f$$

Divide by P_r and rearranging, then

$$\frac{\Delta P_G}{P_r} - \frac{\Delta P_D}{P_r} = \frac{2H}{f^0}\frac{d}{dt}(\Delta f) + \frac{\beta\Delta f}{P_r}$$

$$\Delta P_G(pu) - \Delta P_D(pu) = \frac{2H}{f^0}\frac{d}{dt}(\Delta f) + \beta(pu)\Delta f$$

Taking Laplace transform both sides of equation above

$$\Delta P_G(s) - \Delta P_D(s) = \frac{2H}{f^0}\, s\Delta F(s) + \beta\Delta F(s)$$

$$\Delta F(s) = \frac{\Delta P_G(s) - \Delta P_D(s)}{\frac{2H}{f^0}s + \beta}$$

$$\Delta F(s) = \frac{1}{\beta}\left[\frac{\Delta P_G(s) - \Delta P_D(s)}{\frac{2H}{\beta f^0}s + 1}\right]$$

$$\Delta F(s) = [\Delta P_G(s) - \Delta P_D(s)]\left[\frac{K_{ps}}{1+sT_{ps}}\right] \ldots\ldots\ldots\ldots\ldots\ldots\ldots\ldots \text{(3.2)}$$

Where K_{ps} is power system gain and T_{ps} is power system time constant

$$K_{ps} = \frac{1}{\beta} \;\&\; T_{ps} = \frac{2H}{\beta f^0}$$

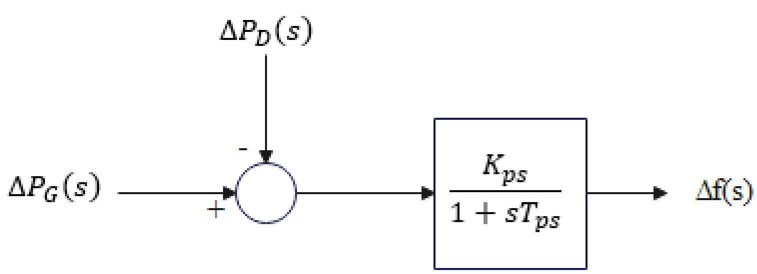

Figure 3.2 Transfer function model of generator load

Governor Model

A sudden increase in electrical load on a generator creates a power imbalance. The generator's rotating parts, like the turbine initially compensate by releasing stored kinetic energy. This, however, causes the turbine and generator to slow down, reducing their rotational speed and consequently, the frequency of the electricity being produced. To counter this, the turbine governor acts like a guardian. It senses the speed change through rotating fly balls and automatically adjusts the turbine's input valve. This adjustment increases the mechanical power output, bringing the speed back to a stable level and restoring the power balance. Interestingly, the first governors, called watt governors, relied on these fly balls for speed detection and used mechanical means to respond to speed variations. However, the majority of current governors employ electrical techniques to detect speed variations. The speed governor system has four essential elements as shown in figure 3.3.

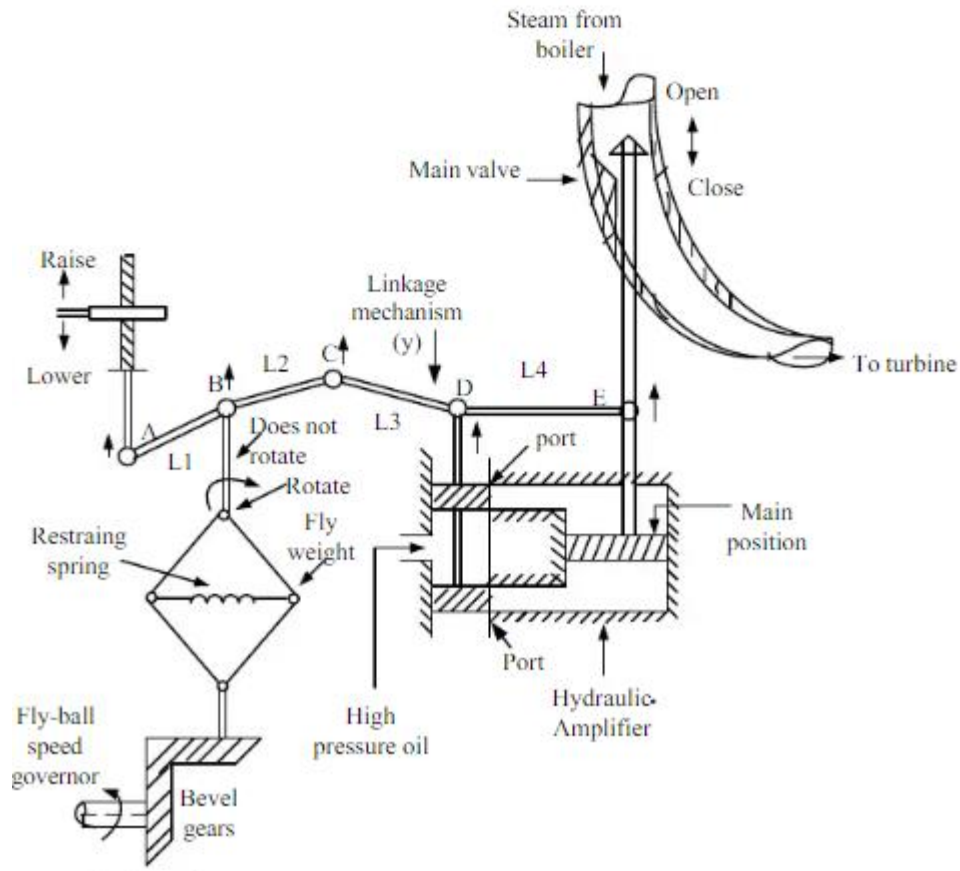

Figure 3.3 Diagram of speed governor system (Sambariya & Fagana, 2017)

The first is the fly ball speed governor, which serves as the system's heart, sensing changes in speed or frequency. As the speed drops, the fly balls travel outwards, while point B on the connection mechanism slides downwards. When speed is reduced, the opposite occurs. The second piece is a hydraulic amplifier, which converts pilot valve action into high-power piston valve movement. This is required to open or close the steam valve against high-pressure steam. The third component is the linkage mechanism, which moves the control valve in accordance to the change in speed and receives feedback from the steam valve movement. The speed changer, the last component, gives the turbine a steady state power output setting for turbine. When it moves downward, the higher pilot valve opens, allowing the turbine to receive more steam while the study is underway. When the speed changer moves upward, the opposite occurs (Sambariya & Fagana, 2017).

By assuming system is originally working in steady state. As a result, the linkage mechanism stationery and pilot valve closed, the steam valve opened by a certain magnitude, and the turbine ran at a constant speed, with the turbine power output balancing the generator load. When the point A in linkage mechanism moved downwards by small amount Δy_A which is a command causes the turbine power output to change and expressed as:

$$\Delta y_A = k_c \Delta P_c \ldots\ldots\ldots\ldots\ldots\ldots\ldots\ldots \text{(3.3)}$$

Where, ΔP_c is the command increase in power

In order to contribute the movement of C either by contributing Δy_A ($-[\frac{L_1}{L_2}]\Delta y_A or - k_1 \Delta y_A$) or by increase change in frequency which causes the fly balls to move outwards so that B moves downwards by a proportional amount of $k_2' \Delta f$. The consequent movement of C with A remaining fixed at Δy_A is:

$$\left[\frac{L_1 + L_2}{L_1}\right] k_2' \Delta f = k_2 \Delta f$$

Therefore, the net movement of C is:

$$\Delta y_C = -k_1 k_C \Delta P_C + k_2 \Delta f \ldots\ldots\ldots\ldots\ldots\ldots\ldots \text{(3.4)}$$

The movement of D Δy_D is the amount by which the pilot valve opens and it is contributed by Δy_C and Δy_E. They can be expressed as:

$$\Delta y_D = \left[\frac{L_4}{L_3 + L_4}\right] \Delta y_C + \left[\frac{L_3}{L_3 + L_4}\right] \Delta y_E$$

$$\Delta y_D = k_3 \Delta y_C + k_4 \Delta y_E \ldots\ldots\ldots\ldots\ldots\ldots\ldots \text{(3.5)}$$

The movement of Δy_D depending up on its sign high opens one of the ports of the pilot valve admitting high pressure oil into the cylinder. The volume of oil allowed to the cylinder is thus proportional to the time integral of Δy_D the movement Δy_E is calculated by dividing the oil volume by the area of the piston's cross section. Thus:

$$\Delta y_E = k_5 \int_0^t -(\Delta y_D)\, dt \ldots\ldots\ldots\ldots\ldots \text{(3.6)}$$

As shown in schematic diagram a positive movement Δy_D, causes negative movement Δy_E. Taking Laplace transform for Δy_E, Δy_D and Δy_C

$$\Delta y_C(s) = -k_1 k_C \Delta P_C(s) + k_2 \Delta f(s)$$

$$\Delta y_D(s) = k_3 \Delta y_C(s) + k_4 \Delta y_E(s)$$

$$\Delta y_E = k_5 \frac{1}{s} \Delta y_D(s)$$

Substituting $\Delta y_C(s)$ and $\Delta y_D(s)$ in to $\Delta y_E(s)$:

$$\Delta y_E = \frac{k_1 k_3 k_C \Delta P_C(s) - k_2 k_3 \Delta f(s)}{k_4 + \frac{s}{k_5}}$$

$$\Delta y_E = [\Delta P_C(s) - \tfrac{1}{R} \Delta f(s)] \times (\tfrac{K_g}{1+sT_g}) \text{………………… (3.7)}$$

Where, R is speed regulation of the governor $R = \frac{k_1 k_C}{k_2}$

K_g is gain of speed governor, $K_g = \frac{k_1 k_3 k_C}{k_4}$

T_g is time constant of speed governor, $T_g = \frac{1}{k_4 k_5}$

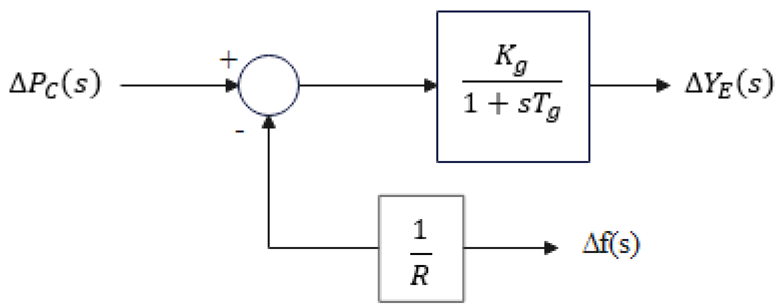

Figure 3.4 Transfer function model of governor

Turbine Model

The source behind power generation comes from the prime mover, which can be a hydraulic turbine using falling water, a steam turbine powered by various fuels like coal, gas, or nuclear, or even a gas turbine. This prime mover connects changes in its mechanical power output $\Delta P_t(s)$ to changes in steam valve position. to adjustments in the steam valve position. It's important to note that different types of prime movers have very different characteristics. For a simple, non-reheat steam turbine, the prime mover can be approximated by a single constant value T_t, this constant captures the relationship between steam valve position and power output. Using this simplification, the transfer function for the system becomes:

$$\frac{\Delta P_t(s)}{\Delta Y_E(s)} = \frac{K_t}{T_t s+1} \dots\dots\dots\dots\dots\dots\dots\dots (3.8)$$

Where, T_t is the turbine time constant and K_t is turbine gain

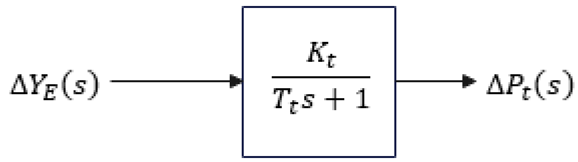

Figure 3.5 Transfer function model of turbine

Two area Automatic Generation Control

Power system can be divided into a number of areas interconnected by means of tie lines. In this area, AGC ensures that power generation across interconnected areas adjusts to meet fluctuating demand while maintaining consistent system frequency. This control system was used to regulate the frequency of each area and simultaneously regulate the tie line power flow between both areas as shown in figure below. Figure 3.6 shows the block diagram of two area AGC system with PID controller.

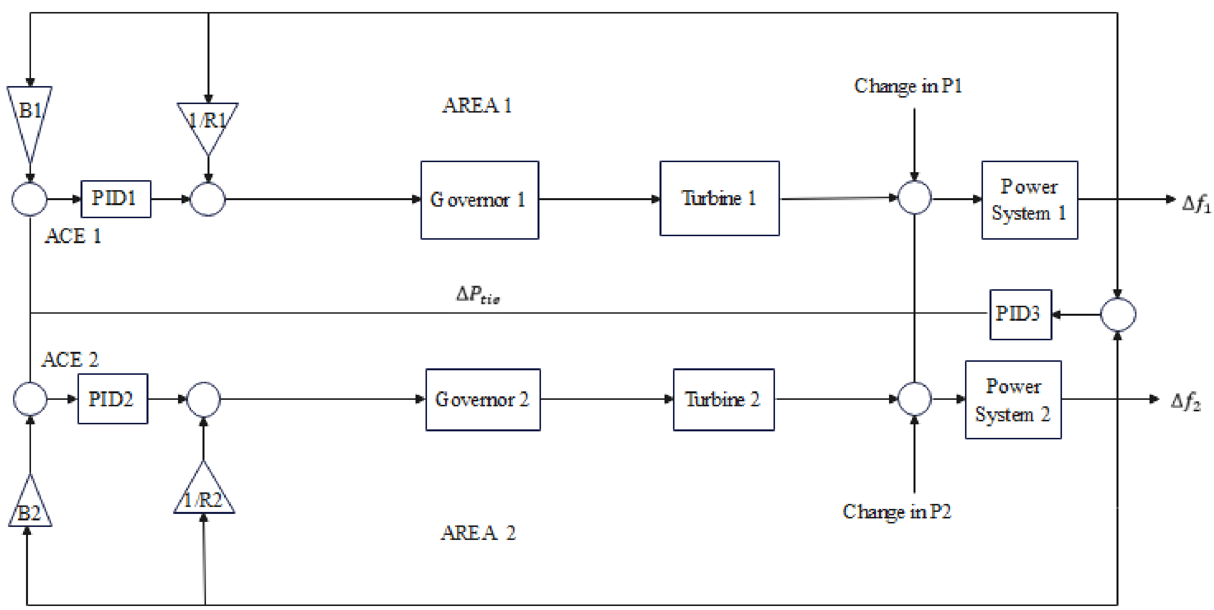

Figure 3.6 Block diagram of two area AGC

3.3.2 PV Model

A photovoltaic model is a mathematical representation of the behavior and performance of solar photovoltaic system, which converts sunlight into electricity through the photovoltaic effect. PV models are used to simulate and analyze the operation of solar panels under different conditions, such as varying levels of sunlight, temperature, shading and system configurations. It includes parameters such as the short circuit current, open circuit voltage, diode ideality factor, series resistance and parallel resistance.

Photovoltaic system is converting the solar energy to electrical when the incident sunlight falls on the surface of the collectors, the photovoltaic currant (Ig) is generated. When the system is in open circuit mode, a potential difference is created, and when it is short circuited, the generated currant (Ig) flows throughout the circuit path, the PN junction equivalent circuit is represented in the figure below.

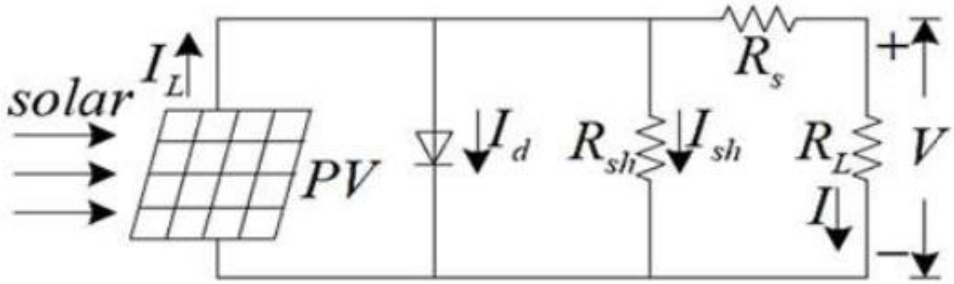

Figure 3.7 Equivalent circuit of PV (Naseri & Ganesh, 2021)

The output of characteristics of PV cell is given as

$$I_{pv} = I_{ph} - I_d - I_{sh} \text{………………….. (3.9)}$$

$$I_{pv} = I_{ph} - I_o\left(e^{q(V_{pv}+\frac{I_{pv}R_{S})}{AKT}} - 1\right) - \frac{V_{pv}+I_{pv}R_s}{R_{sh}} \text{……….. (3.10)}$$

Where, I_{pv} *and* V_{pv} are the output current and voltage respectively, I_{ph} is the photocurrent, I_d is the diode junction current, I_o is the reverse saturation current, q is the electronic charge, K is the Boltzmann constant, T is the PV cell temperature, A is the diode factor and R_s and R_{sh} are the PV cell series and parallel resistance respectively.

I_{ph} or photocurrent can be described as the following equation:

$$I_{ph} = (I_n + K_I\Delta T)\frac{G}{G_n} \text{………………….. (3.11)}$$

Where, I_n is the current under the normal condition, K_I is the short circuit current per temperature factor, ΔT is the temperature difference between the actual and nominal values, G *and* G_n the solar irradiation and its nominal value respectively. Figure below shows the I-V curve originated from the above equation with three remarkable points: short circuit (0, I_{sc}), maximum power point (V_{mp}, I_{mp}) and open circuit (V_{oc}, 0).

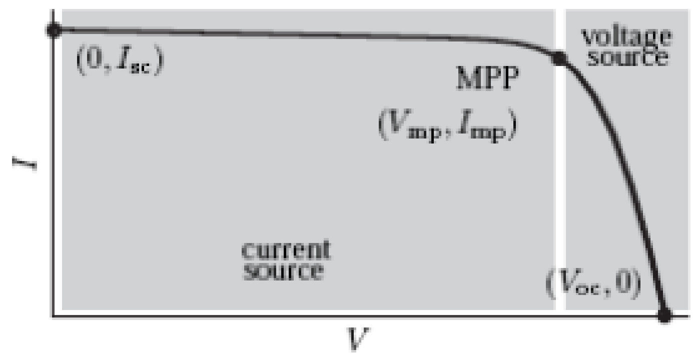

Figure 3.8 Characteristic I-V curve of PV cell

The output power (in watts) of the PV system is determined by:

$$P_{pv} = \eta S\Phi\{1 - 0.005(T_a + 25)\} \qquad (3.12)$$

Where, P_{pv} is power output from the PV

η is the conversion efficiency of the PV array, ranging between 9%-12%

S is the measured area of the PV array/$S = 4084m^2/1$

Φ is the solar radiation, $\Phi = 1kW/m^2$

T_a is ambient temperature in degree Celsius

For this thesis, A Metehara Solar Power PV Plant is chosen for this thesis which is under project in the Oromia region, Ethiopia (Power, 2019). These plants have 100MW rating and integrated to the system model. So, both areas are assumed to have a 100MW photovoltaic (PV) power plant. The electrical characteristics of this plant are detailed in Table 3.1. To facilitate the modeling process, the converter and inverter are combined and represented as a first-order transfer function.

Table 3.1 Characteristics of the PV power plant (Power, 2019)

Power	100MW
Irradiation	$1000W/m^2$
Temperature	25ºC
Air Mass	1.5
DC output under STC	100Wp-350Wp

PV in Automatic Generation Control

AGC in PV systems is essential for managing the integration of solar energy into power systems. PV systems generate electricity from sunlight and their output is subjected to variations in solar irradiance levels, cloud cover and other environmental factors. So AGC plays a crucial role in maintaining stability by adjusting the power output of PV to match system demand and ensure frequency and voltage regulation. The design of AGC controllers often involves analyzing the transfer functions of the power system components to understand their dynamic response characteristics and determine the appropriate the control parameter.

The transfer function of PV systems represents the relationship between input and output of PV which quite complex due to the nonlinear characteristics of PV panels and the influence of environmental factors. Transfer functions involves starting with the electrical characteristics of the PV system, considering the solar irradiance, temperature effects and the electrical conversion process. Linearization of the equations around an operating point allows for the representation in terms of a transfer function.

The Power output from the PV system is linearized as:

$$\Delta P_{pv} = G_{pv}\Delta S \ldots\ldots\ldots\ldots\ldots\ldots\ldots\ldots\ldots.. (3.13)$$

Where, G_{pv} is the transfer function of PV system. So, a simplified representation of the transfer function for PV are represented as follows:

$$G(s) = \frac{P_{out}(s)}{S_{in}(s)} = \frac{K_{pv}}{1+sT_{pv}} \ldots\ldots\ldots\ldots\ldots\ldots\ldots (3.14)$$

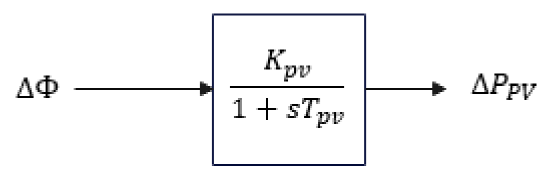

Figure 3.9 Transfer function model of PV

Where, $P_{out}(s)$ is Laplace transform of the PV power output, $S_{in}(s)$ is Laplace transform of solar input to the PV system, K_{pv} is the gain and T_{pv} is the time constant

3.3.3 Wind Turbine Model

In the WT system, turbine blades transform wind energy into kinetic energy. The aerodynamic rule approximates the link between wind speed and turbine power using the following equation:

$$P_t = \frac{1}{2} C_P(\lambda, \beta)\rho A V_\omega^3 \ldots\ldots\ldots\ldots\ldots\ldots (3.15)$$

Where, ρ is the air density, A is the blade sweep area, V_ω is the wind speed, C_P is the power coefficient, β is pitch angle and λ is tip speed ratio.

The tip speed ratio is represented by the following equation:

$$\lambda = \frac{\omega_t r}{V_\omega}$$

Where, ω_t is the turbine rotor speed and r is the rotor radius.

The pitch angle control strategy is established by adjust the value of *Cp* that aims at maximizing the output power of the turbine. *Cp* is determined by the aerodynamics design and it can be approximated by the following equation:

$$C_P(\lambda, \beta) = C_1(\frac{C_2}{\lambda_i} - C_3\beta - C_4\beta^{C_5} - C_6)e^{C_7/\lambda_i} \ldots\ldots\ldots\ldots\ldots (3.16)$$

Where:

$$\frac{1}{\lambda_i} = \frac{1}{\lambda + 0.08\beta} - \frac{0.035}{\beta^3 + 1}$$

In this thesis, Adama I wind farm is chosen with 51 MW which is located at Adama, Ethiopia. So, this wind farm was connected to the two-areas, as shown in block-diagram. This farm includes 34 wind turbines with each of 1.5 MW rated capacity and have data as shown in table form in appendix (Kebede et al., 2016). The pitch angle controller is utilized to get maximum power point tracking conditions. So, the power coefficient calculated from power is given as follows:

$$C_P * \frac{1}{2} * 0.97\frac{kg}{m^3} * 4654\ m^2 * (11m/s)^3 * 0.5 = 1.5\ MW$$

$$C_P = 0.5$$

To find λ_i, we use

$$\frac{1}{\lambda_i} = \frac{1}{\lambda + 0.08\beta} - \frac{0.035}{\beta^3 + 1}$$

$$\frac{1}{\lambda_i} = \frac{1}{6.14 + 0.08 * 0} - \frac{0.035}{0^3 + 1}$$

$$\lambda_i = 7.82$$

Then the value of turbine rotor speed ω_t, $\lambda = \frac{\omega_t r}{V_\omega}$

$$\omega_t = \frac{\lambda V_\omega}{r}$$

$$\omega_t = \frac{7.82 * 11}{38.5}$$

$$\omega_t = 2.234$$

Wind in Automatic Generation Control

AGC in wind turbines is a crucial aspect of managing the integration of wind energy into power systems. Wind turbines subjected to fluctuations in wind speed and direction resulting in variable power output. AGC plays a key role in maintaining stability by adjusting the power output to meet system demand and ensure frequency and voltage regulation. The transfer function of a wind turbine represents the relationship between the input (wind speed or wind direction) and output (generated electrical power or rotor speed) of the wind turbine system.

The transfer function of wind turbine was quite complex because of the nonlinear aerodynamic characteristics of the rotor blades, mechanical dynamics of the drive train control strategies implemented in the system. A simplified linear transfer function can be used in this thesis to approximate the dynamic response of a wind turbine under certain operating conditions. To simplify the modeling of the wind farm, the wind turbines are modelled and depicted as follows:

$$G(s) = \frac{K_{wt}}{(T_{wt}s+1)} \ldots\ldots\ldots\ldots\ldots\ldots (3.17)$$

Where, $\boldsymbol{K_{wt}}$ is overall gain of the system and $\boldsymbol{T_{wt}}$ time constants of wind turbine. The variables of the wind farm are presented in Table 3.2.

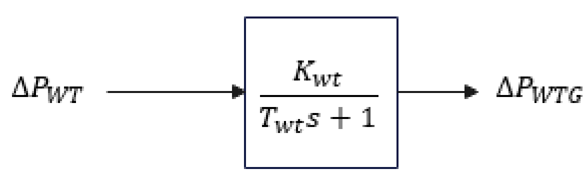

Figure 3.10 Transfer function model of wind

Table 3.2 Parameters of renewable energy source model of PV and wind

Parameter	Value
K_{wt}	1
K_{pv}	0.3s
T_{wt}	1
T_{pv}	0.01s

3.3.4 Vanadium Redox Flow Battery Model

Vanadium redox flow batteries (VRBs) are emerging as a compelling solution for large-scale energy storage due to their attractive properties. These batteries boast independent scalability of power and energy capacity, alongside high efficiency and long durations of energy storage.

Modelling VRBs using transfer functions provides a powerful tool for understanding and optimizing their dynamic behavior in various applications. By representing the VRB's complex electrochemical processes through a transfer function, researchers and engineers can gain valuable insights into the battery's performance under different operating conditions. This modelling approach facilitates the design of improved control systems, ultimately enabling the VRFB to reach its full potential in energy storage applications.

In recent years different types of VRFB are manufactured with different output power. The output power of this battery is improved time to time and move toward megawatt scale (1 MW and above). In this thesis, a INVINITY VS3-022 VRFB manufactured by INVINITY energy systems company with the rated energy storage capacity of 78 KW was integrated to the two-area power system. The overall parameter specifications of the battery are shown in appendix.

VRFB in Automatic Generation Control

AGC in VRFB system involves controlling the charging and discharging process of the battery to respond fluctuations in renewable energy generation. The AGC system continuously monitor the state of charge of the VRFB and adjusts the charging and discharging current to maintain the desired operational parameter. Generally, the transfer function of VRFB in the context of automatic generation control with renewable energy systems involves linearizing the electrochemical model of the VRFB and then integrating it with the AGC system. The block diagram of VRFB energy storage system is shown in figure 3.11.

As shown in the block diagram, VRFB was worked like a dual converter, i.e., both rectifier and inverter action. The battery will be charged during low load conditions and it will be discharged or delivers the energy during sudden load perturbations. In AGC system, ACE is being used directly as the input signal to VRFB.

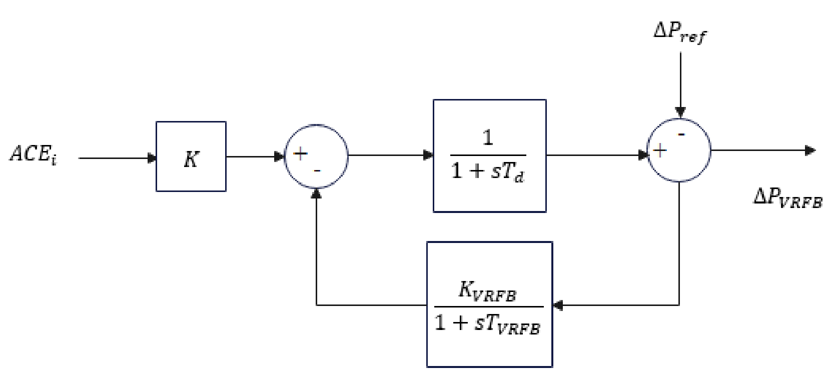

Figure 3.11 Transfer function model of VRFB

The simplified representation of the transfer function:

$$G(s) = \frac{K_{VRFB}}{T_{VRFB}+1} \ldots\ldots\ldots\ldots\ldots\ldots\ldots\ldots (3.18)$$

Where, K_{VRFB} is gain of VRFB and T_{VRFB} is time constant of the VRFB.

3.3.5 Flywheel Energy Storage System Model

Flywheel energy storage systems (FESS) are gaining traction due to their ability to deliver rapid bursts of power. They are ideal for applications requiring high-power output for short durations. Modelling FESS using transfer functions allows for the analysis and design of control systems that optimize their performance and integration into power grids. This approach simplifies the complex dynamics of the FESS while capturing its essential characteristics for control design purposes. The energy stored by the flywheel can be expressed as:

$$E = \frac{1}{2} J \omega^2 \ldots\ldots\ldots\ldots\ldots\ldots\ldots\ldots (3.19)$$

Where, E is the Energy stored in the flywheel in N-m, J is the flywheel moment of inertia in N-m-sec^2, and ω is the rotational velocity in rad/sec.

The amount of energy stored by the flywheel is indicated by the speed of its flywheel rotor, so the maximum value of its stored energy is calculated by the maximum and minimum flywheel rotor speeds, so:

$$E_{max} = \frac{1}{2} J(\omega_{max}^2 - \omega_{min}^2)$$

In recent years FESS are manufactured by different electrical power companies. In this thesis a flywheel energy storage manufactured by Beacon Power is integrated to the two-area power systems. This FESS have capacity of 100 KW per flywheel and other specification of the parameters are as shown in the appendix.

Flywheel Energy Storage in Automatic Generation Control

Flywheel energy storage system can help in AGC by providing fast response times, high efficiency and reliable frequency regulation capabilities. And also enhance stability, improve frequency control and support integration of renewable energy resources into power systems. The transfer function of a flywheel in hybrid renewable energy system was derived based on the rotational dynamics of the flywheel. A simplified second order transfer function was often used to model the behavior of a flywheel. The rotational motion of a flywheel can be described by differential equation:

$$J\frac{d^2\theta}{dt^2} + b\frac{d\theta}{dt} + k\theta = T \text{……………………. (3.20)}$$

Where, J is moment of inertia of the flywheel, b is damping coefficient, k is the stiffness (spring) constant, θ is angular displacement and T is external torque applied to the flywheel.

Assuming small angular displacement, neglecting the stiffness term and dividing by J

$$\frac{d^2\theta}{dt^2} + \frac{b}{J}\frac{d\theta}{dt} = \frac{T}{J}$$

Now let $\omega = \frac{d\theta}{dt}$ which is the angular velocity. Then the equation becomes:

$$\frac{d\omega}{dt} + \frac{b}{J}\omega = \frac{T}{J}$$

Taking the Laplace transform assuming zero initial condition:

$$s\Omega(s) + \frac{b}{J}\Omega(s) = \frac{T(s)}{J}$$

Where $\Omega(s)$ is the Laplace transform of ω

By rearranging the transfer function G(s):

$$G(s) = \frac{\Omega(s)}{T(s)} = \frac{1}{s+\frac{b}{J}} \text{……………………. (3.21)}$$

Generally, the transfer function of flywheel in the context of automatic generation control with renewable energy systems involves combining the rotational dynamics of the flywheel with dynamics of AGC system. The function starts with the rotational dynamics of flywheel and linearizing the equations around a nominal operating point. The Flywheel Energy Storage System (FESS) model consists of two key parts: the flywheel governor and the flywheel device model. The FESS model is represented by a first-order transfer function, which essentially mimics the dynamic interaction between the FESS and the power system. This transfer function has a time constant T_{FESS} of 0.015 seconds, indicating how quickly the FESS responds to changes in the power system's demands.

$$G(s) = \frac{1}{T_{FESS}s+1} \text{……………………. (3.22)}$$

The flywheel governor acts as the brain of the FESS. It receives the Area Control Error (ACE) signal as input, which reflects the power imbalance in the system. Based on this information, the governor calculates a power setpoint signal as output. This setpoint essentially tells the flywheel how much power it needs to either deliver to the power system (positive value) or absorb from the system (negative value) to help maintain grid stability. The governor's decision-making process hinges on the difference between the mechanical torque generated by the flywheel's rotation and the electrical torque demanded by the power system. In simpler terms, it compares how much power the flywheel is currently producing versus how much power the grid needs.

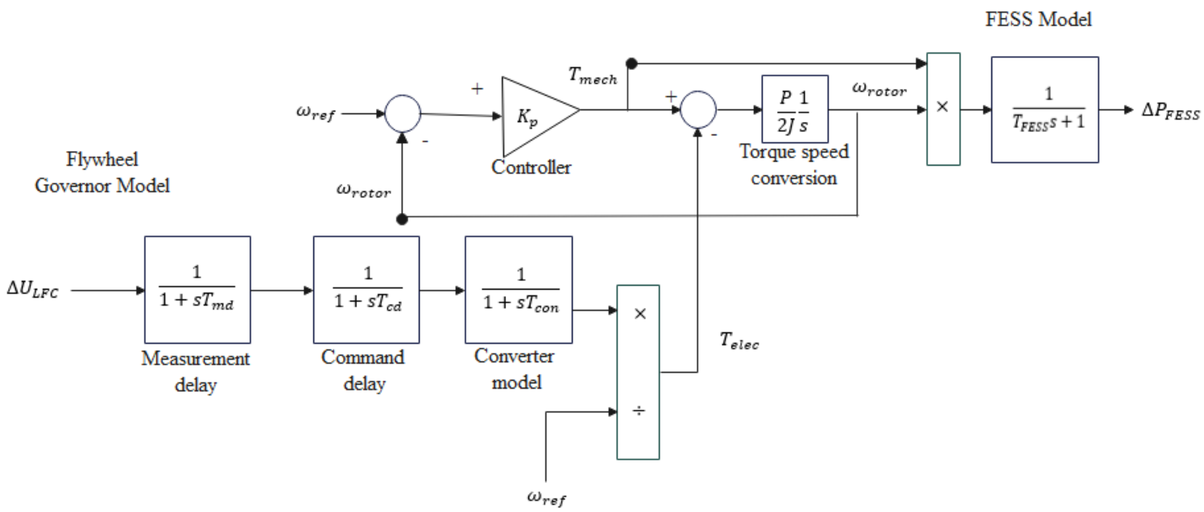

Figure 3.12 Transfer function model of FESS

A key factor in the FESS's performance is the angular speed of its rotor. This speed dictates how much rotational energy is stored (higher speed means more stored energy) and how quickly the system can deliver or absorb power. To enhance the accuracy of simulating the FESS's dynamic behavior as shown in figure 3.12, angular speed control is incorporated into the proposed model. Another important concept is rotor angular acceleration. This measures how rapidly the rotor speeds up or slows down as energy is exchanged with the power system. In other words, it reflects the rate of change in the rotor's speed. The equation for rotor angular acceleration in the time domain is as follows:

$$\frac{d\omega_r}{dt} = \frac{P}{2}\left(\frac{T_{elec}-T_{mech}}{J}\right)\ldots\ldots\ldots\ldots\ldots\ldots\ldots\ldots (3.23)$$

Applying Laplace transform both side:

$$\omega_r = \frac{P}{2}\left(\frac{T_{elec}(s) - T_{mech}(s)}{Js}\right.$$

Then the electrical torque can be computed as:

$$T_{elec} = \frac{P_{elec}}{\omega_{ref}} \ldots\ldots\ldots\ldots\ldots\ldots\ldots\ldots\ldots (3.24)$$

The shaft mechanical torque can be computed as follows:

$$T_{mech} = K_p(\omega_r - \omega_{ref}) \ldots\ldots\ldots\ldots\ldots\ldots (3.25)$$

Where, ω_r denotes the angular speed of the rotor (rad/s), ω_{ref} is the reference electrical frequency (rad/s), *P* is the number of poles, *J* is the inertia of the rotating masses ($kg.m^2$), the symbols T_{md} , T_{cd} and T_{con} represents the time constants of measurement delay, command delay and converter respectively.

This transfer function of a flywheel energy storage system (FESS) isn't perfect. It incorporates parameters like measurement delay, command delay and converter delay to account for these imperfections. These delays represent the time it takes for different parts of the system to react. Measurement delay reflects the lag between a physical change in frequency and its conversion to a usable signal. Command delay captures the processing time for the control system to decide on a response. Finally, converter delay represents the time needed for the motor-generator to translate electrical signals into action on the flywheel. Including these delays in the transfer function is crucial for non-idealities, the transfer function provides a more realistic picture of the FESS, paving the way for effective control and optimal system performance. Table 3.3 shows parameter values of transfer function of the flywheel energy storage system which used in the simulation part, these values are gathered from reviewed literatures and from the selected flywheel energy storage specifications shown in appendix.

Table 3.3 Parameters of time constants of FESS

Parameter	Value
T_{con}	0.1
T_{cd}	0.01
T_{md}	0.1

3.3.6 Proportional Integral Derivative Controller

PID controller is usually used in the industrial applications control system as control loop feedback. This PID controller continuously monitors the process variable and compares it to the set point to determine the error. Based on this error signal, the PID controller calculates the control output that is sent to the actuator to adjust the process and bring the process variable closer to the setpoint (Ang, K.H., Chong, G. and Li, 2007). PID controller have three main components:

- Proportional (P) term responds to the current error between the desired setpoint and the actual processes variable, $P_{out} = K_p e(t)$
- Integral (I) term considers the accumulation of past errors over time to eliminate any steady state error, $I_{out} = K_i \int_0^t e(t)\, dt$
- Derivative (D) term predicts future error based on the rate of change of the error, $D_{out} = K_d \frac{d}{dt} e(t)$

In this thesis PID controller is used because of they can quickly respond to changes in system frequency or load demand, they help to maintain system stability by adjusting the power output to match the load demand, they are versatile and robust in the power system, they offer flexibility in tuning parameters in order to optimize system performance and finally its simplicity to calculate the gain. They can improve the dynamic performance and minimize the steady-state error. The value of gains K_p, K_i and K_d were automatically achieved by a correction in the MATLAB simulation model. K_p is used to decrease the rise time, K_d is used to decrease the overshoot and settling time and K_i is to remove the steady-state error.

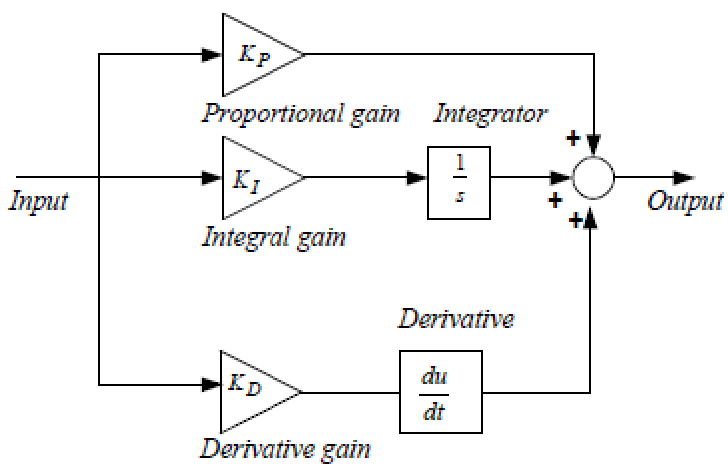

Figure 3.13 Structure of PID Controller

The transfer function of the controller can be expressed mathematically as follows:

$$G_C(s) = k_p + \frac{k_i}{s} + k_d * \frac{N}{\frac{N}{s}+1} \ldots\ldots\ldots\ldots\ldots\ldots (3.26)$$

Where, k_p is proportional gain which multiplies error signal, reducing rise time for a faster response but potentially increasing overshoot and instability at high values. k_i is integral gain integrating the error signal, eliminating steady-state error but potentially increasing overshoot and settling time. k_d is the derivative coefficient which is multiplies the derivative of the error signal, damping the response and improving stability, but potentially introducing high frequency oscillations. A filter with adjustable coefficient N helps dampen these oscillations (Ang, K.H., Chong, G. and Li, 2007).

3.3.7 Overall model of the proposed system

The overall model of this thesis consists of two area interconnected power system including renewable energy sources and energy storage system. Those RES and ESS are designed one by one as showed in above discussion, they come to one interconnected system as shown in figure 3.14. This two-area interconnected system are connected by using tie line and also used PSO based PID controller for controlling strategy. In area 1 there is step load perturbation in order to see performance of the system under load variability. PV and winds are the renewable energy sources chosen in the system because they are more uncertain than other renewables energies. From energy storage system vanadium redox flow battery and flywheel energy storage are included in the model to store and release the energy when needed depend on the power generated.

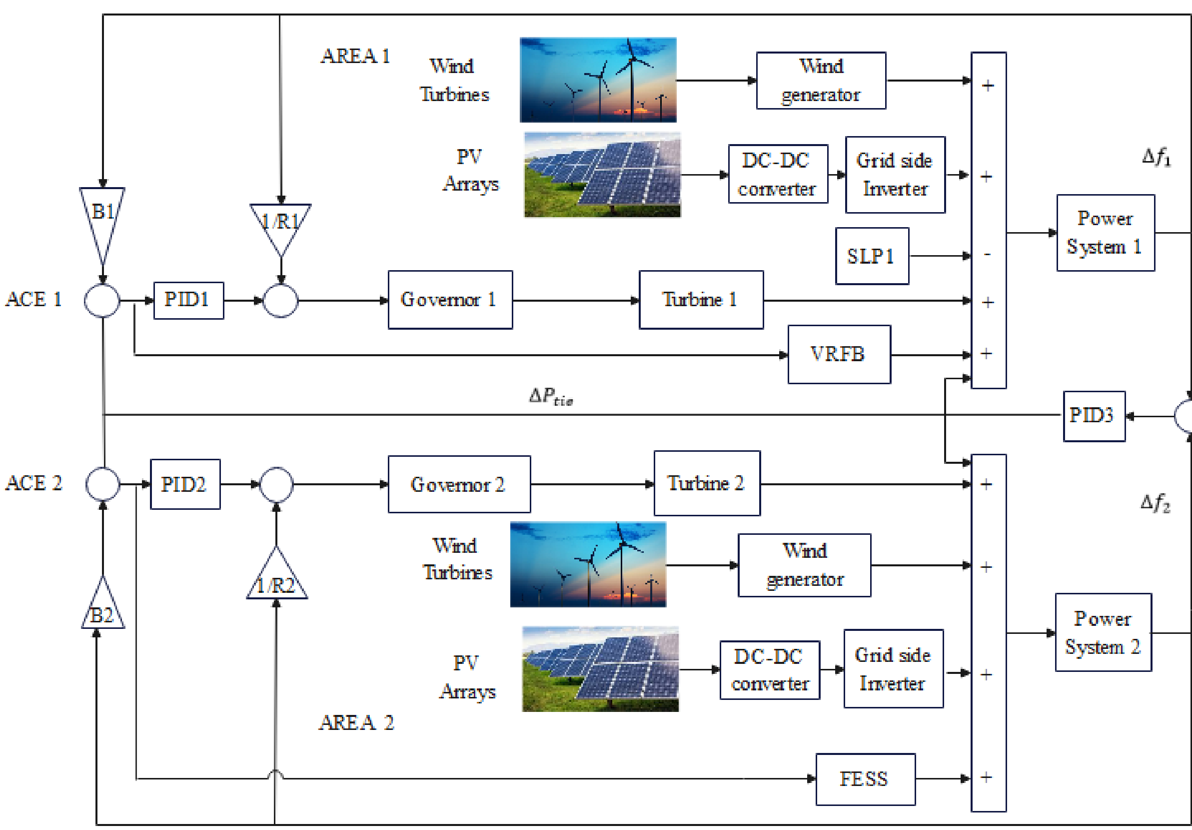

Figure 3.14 Block diagram of proposed interconnected power system including RES and ESS

3.3.8 Case Study Analysis

Each control area has total power capacity of 1000 MW and 2000 MW respectively. The base power of each area was 1000 MVA and 2000MVA respectively with power system frequency of 50 Hz. In this model PV power, wind power, vanadium redox flow battery and flywheel energy storage are integrated to the power system with thermal power plant. PV power plant was integrated to the power system model in area-1 and area-2. In order to get real data of solar power, A 100 MW rating of Metehara Solar Power PV Plant is chosen for this thesis which is under project in the Oromia region, Ethiopia (Power, 2019). Integrating a photovoltaic (PV) power plant to the power system requires two key components: a converter and an inverter. The converter acts as an optimizer, ensuring the PV system operates efficiently. It does this by managing the power flow within the PV plant itself. Meanwhile, the inverter plays a crucial role in voltage conversion. It converts the DC (direct current) electricity generated by the solar panels into AC (alternating current) electricity that matches the power system AC voltage. For the purposes of simulation, both areas in this study are assumed to have a 100MW PV power plant and the converter and inverter are combined and modeled as a first-order transfer function. The detailed electrical characteristics of these plants are provided in the appendix.

Wind power was another renewable energy which integrated to the power system, Adama I wind farm is chosen with 51 MW rating which is located at Adama, Ethiopia to be integrated to the system model. This wind farm has 34 wind turbines with each of 1.5 MW rated capacity and have electrical and mechanical data as shown in appendix. From the energy storage system, a 20 MW capacity of flywheel energy storage was integrated to the area-2 and a 30 MW capacity of vanadium redox flow battery was integrated to the area-1. For both energy storage system, the characteristics and specifications of each parameter was shown in appendix as gained from their manufacturer. The parameters assumed for the proposed two area interconnected power system controlled by AGC system with the integrated RES and ESS are as shown in Table 3.4. All the output power of the RES and ESS used as per unit in the proposed power system because of per unit in AGC simplifies analysis, facilitates control system design and provides a common basis for comparing and evaluating different components within the power system.

Table 3.4 Parameters of the proposed system model

Parameters	Area 1	Area 2
Normal Operating Load	1000 MW	2000 MW
Frequency	50	50
Inertia Constant (H)	5	4
Speed Regulation (R)	0.05	0.0625
Governor Time Constant	0.2	0.3
Turbine Time Constant	0.5	0.6
Frequency sensitive load coefficient (D)	0.6	0.9
PV power	100 MW	100 MW
Wind power	51 MW	51 MW
FESS	-	20 MW
VRFB	30 MW	-

The base power of Area 1 is 1000MW and the power change occur in area 1 is 200MW. Then the per unit value ΔP_{d1} which is power change in area 1 calculated as:

$$\Delta P_{d1} = {}^{200MW}/_{1000MW} = 0.2\ pu$$

Frequency bias constant of the control area was calculated as:

$$\beta_1 = {}^{1}/_{R_1} + D_1 \text{………………………..} \quad (3.27)$$

$$\beta_1 = 0.6 + \frac{1}{0.05} = 20.6\ MW/Hz$$

$$\beta_2 = {}^{1}/_{R_2} + D_2$$

$$\beta_2 = 0.9 + \frac{1}{0.0625} = 16.9\ MW/Hz$$

The per unit steady state frequency deviation is:

$$\Delta\omega_{ss} = \frac{-(\Delta P_{d1}+\Delta P_{d2})}{({}^{1}/_{R_1}+D_1)+({}^{1}/_{R_2}+D_2)} = \frac{-(\Delta P_{d1}+\Delta P_{d2})}{\beta_1+\beta_2} \text{……………} \quad (3.28)$$

$$\Delta\omega_{ss} = -\frac{0.2}{20.6+16.9} = -0.00533\ pu$$

The steady state frequency deviation in Hz is:

$$\Delta F = (-0.00533)(50) = -0.2666\ Hz$$

The new frequency is:

$$F = \Delta F + f_0 = 50 - 0.2665 = 49.733\ Hz$$

The change in mechanical power in area 1and 2 is:

$$\Delta P_{m1} = {}^{\Delta\omega_{ss}}/_{R_1} = {}^{-0.00533}/_{0.05} = 0.1066\ pu = 106.6\ MW$$

$$\Delta P_{m2} = {}^{\Delta\omega_{ss}}/_{R_2} = {}^{-0.00533}/_{0.0625} = 0.08528\ pu = 85.28\ MW$$

Therefore, area-1 increased the generation by 106.6 MW and area-2 by 85.25 MW with a new operating frequency of 49.733 Hz. The total power change in generation is 191.88 MW, which is 8.12 MW less than the 200 MW load change because of frequency drop.

The tie line power flow is:

$$\Delta P_{12} = \Delta\omega_{ss}({}^{1}/_{R_2} + D_2) \ldots\ldots\ldots\ldots\ldots\ldots\ldots\ldots.. (3.29)$$

$$\Delta P_{12} = (-0.00533)(16.9) = -0.09\ pu = -90\ MW$$

Rotating mass and load of both areas are calculated as:

$$Area\ 1 = \frac{1}{2H_1 s + D_1} = \frac{1}{2 * 5s + 0.6} = \frac{1}{10s + 0.6}$$

$$Area\ 2 = \frac{1}{2H_2 s + D_2} = \frac{1}{2 * 4s + 0.9} = \frac{1}{8s + 0.9}$$

The objective function of the optimization problem relies on the ITAE criterion, which can be formulated as follows:

$$ITAE = \int_0^{t_s} (|\Delta F_1| + |\Delta F_2| + |\Delta P_{tie}|) . t . dt \ldots\ldots\ldots\ldots\ldots (3.30)$$

Where, $\Delta F_1$and ΔF_2 are the frequency deviation of area-1 and 2 respectively, ΔP_{tie} is the tie line power change between the two-areas *1* and *2*, and t_s is simulation time.

3.3.9 Particle Swarm Optimization

Overview of PSO Technique

Particle Swarm Optimization method (PSO) is an alternate approach to solving the challenging non-linear optimization problem and a revolutionary population-based stochastic search algorithm. The PSO algorithm's core concept was initially inspired by simulations of animal social behavior, such as flocking behavior in birds and fish schools. PSO was first presented by Drs. Kennedy and Eberhart in 1995. It is based on the way that groups of birds or insects naturally communicate with one another to exchange individual knowledge when they migrate or look for food in a certain area, even though none of them is aware of the optimal location.

However, from the nature of social behavior, if any member can identify a desired course of action, the rest of the members will follow quickly (Talukder, 2011).

In order to solve optimization problems, the PSO algorithm essentially learns from the actions or behaviors of animals. In PSO, the population is referred to as a swarm, and each individual within it is called a particle. Beginning with a population that has been randomly initialized, each particle traverses the searching space while remembering its best past positions as well as those of its neighbors, moving in randomly selected directions. A swarm's particles can dynamically modify their own position and velocity based on the best position of all the particles in addition to communicating good positions to one another. When every particle has been transferred, the following phase starts (Li et al., 2021).

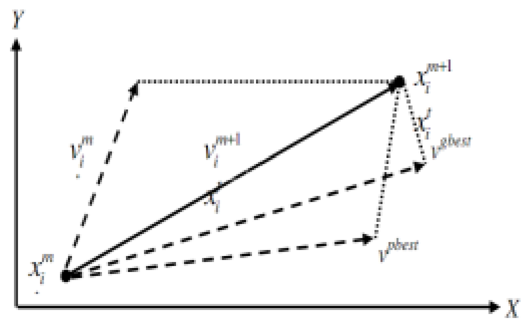

Figure 3.15 Concept of searching of particles (Shaikh & Yadav, 2022)

Particle Swarm Optimization is an attractive option for Automatic Generation Control (AGC) due to its inherent ability to strike a balance between exploration and exploitation in complex optimization landscapes PSO's population-based method works well in the field of AGC, where dynamic power system conditions require effective controller parameter tweaking. PSO provides a strong foundation for determining the optimal or nearly optimal settings for AGC controllers by concurrently examining several parts of the parameter space and taking use of viable solutions (Shaikh & Yadav, 2022).

This thesis leverages Particle Swarm Optimization (PSO) due to its several advantages. Firstly, PSO is known for its ease of implementation. It doesn't require complex calculations or gradient information about the function being optimized, making it user-friendly. Secondly, it utilizes basic mathematical operations, further contributing to its simplicity. These factors combined often lead to fast convergence, meaning the algorithm finds a good solution quickly. Beyond its ease of use, PSO boasts strong performance**.** Compared to other optimization methods, it can deliver solutions faster, with lower computational cost, and greater overall efficiency. This makes it a cost-effective and powerful tool for various optimization problems. Furthermore, PSO offers flexibility. With only a few adjustable parameters, it can be adapted to tackle a wide range of problems, including those with non-linear, non-convex functions, and those involving continuous, discrete or even integer variables**.** This versatility makes PSO a highly attractive choice for a wide variety of optimization tasks.

Components and Optimization of PSO

The purpose of optimization is to find the best value for the vector $X = [x_1\ x_2\ x_3/1x_n]$ which represents a variable in the stated issue. The variable X is an n-dimensional vector known as a position vector, where n is the number of variables to be determined by the optimization process. An objective function, also known as a fitness function, is used to judge the solution obtained during the optimization process. Consider a swarm made up of p particles. The position vector X and velocity vector V are used to represent the position and velocity of each particle in the swarm at a given iteration. (Talukder, 2011).

$$X_j^t = [x_{j1}\ x_{j2}\ x_{j3}/1x_{jn}] \ldots\ldots\ldots\ldots\ldots\ldots \text{(3.31)}$$

The position vector X_j^t gives the position of j^{th} particle in n- dimensional search space at t iteration.

$$V_j^t = [v_{j1}\ v_{j2}\ v_{j3}/1v_{jn}] \ldots\ldots\ldots\ldots\ldots\ldots\ldots\ldots \text{(3.32)}$$

Velocity vector V_j^t represents velocity of particle j at t iteration. A particle j is defined by its velocity vector v_j and position vector X_j.

The movement of every particle in the search space in affected by its own best position called as local best compared to previous positions attained so far by the particle and is given as $pbest_{jk}$. Here, $j = 1,2, \ldots., P$ and $k = 1,2, \ldots, n$. Similarly, the best position attained so far by the swarm as a whole regardless of which particle has achieved, is called as global best and is given as $gbest_j$. The position and velocity vectors are updated through dimensions k as per the following equations:

$$X_{jk}^{t+1} = X_{jk}^t + V_{jk}^{t+1}$$

The above equation is used for updating particle's position.

$$V_{jk}^{t+1} = \omega V_{jk}^t + c_1 r_1 \left(pbest_{jk} - X_{jk}^t\right) + c_2 r_2 (gbest_j - X_{jk}^t)$$

According to the above equation, there are three primary elements that affect the movement of particles in the swarm during an iteration. The inertia weight constant (ω) which is a positive constant value. The particle's search is said to remain constant while continuing in the direction of its previous motion. The balance between local search known as exploitation and global search known as exploration are also maintained by the inertia constant. The particle velocity in the previous direction is indicated by the value of ω=1.

The second component of the above equation is termed as the cognition term. The cognitive term in PSO influences a particle's movement towards its own best-found position. It considers the difference between the particle's current position and its personal best. As this difference increases (particle strays further from its best position), the cognitive term strengthens, guiding the particle back towards its past success.

The social term is influenced by the social learning coefficient c_2, which balances the impact of the swarm's knowledge. Similar to the cognitive coefficient, c_2 is typically set within a range to maintain a balance between individual and collective learning. The role of r_2 is same as that of r_1 (Dhawane & Bichkar, 2020).

Steps to tune PID Controller with PSO

Designing of a PSO based controller involves leveraging the optimization capabilities of PSO to tune the parameters of the controller for optimal performance in controlling complex systems. A performance index is a quantifiable metric used to evaluate a system's behavior. By choosing an appropriate performance index, optimal performance against desired specifications was achieved by adjusting system parameters. This systematic approach ensures the system meets design goals efficiently. The design involves several key steps to develop an effective optimization technique. Here are the steps involved in the design of a PSO algorithm used in this thesis.

1. The conventional PID controller sets minimum and maximum gain boundaries of PID controllers. The starting particle matrix is created by selecting a value with a uniform probability from the search space ($gmin$=0, $gmax$ =1).
2. The initial values of particle velocities are set to zero.
3. The initial particle swarm was assessed by simulating the automatic generation control model with each particle's gains applied as the PID controller settings. A performance index (ISE/ITAE) is then calculated for each particle to evaluate its effectiveness.
4. Initialize $pbest$ for each particle.
5. Find the $gbest$ based on the minimum performance index in initial particle matrix.

6. Start the iteration, $iter = 1$.
7. Update the velocity of the particle by help of the equation provided below:

$$Velocity = C \times (\omega \times velocity + c_1 \times r_1 \times (pbest - particle) + c_2 \times r_2 \times ((ones(N,1) \times gbest) - particle))$$

   Where: $C = 1, c_1 = 1, c_2 = 4 - c_1, \omega = \frac{\max iter - iter}{\max iter}, r_2 \& r_1$ are the random numbers
8. By using updated velocity, create new particle
9. If a new particle’s position exceeds the search space boundaries, then select one and generate new values that ensures the exploration stays within the defined particle search space.
10. Determine performance index value for new particle using the simulation of AGC block model.
11. Update each particle's best local location ($pbest$) by comparing the minimum value of the new particle performance index to the previous $pbest$ performance index.
12. Update $gbest$ global minimum particle and its performance index.
13. $Iter = iter + 1;$
14. If $iter \leq max\ iter$ go to where the velocity was updated, unless go to next step.
15. Finally, $gbest$ controller gain values with its performance index value were printed.

The convergence curve typically shows how the fitness value changes over iterations as the PSO algorithm searches for optimal PID controller gains.

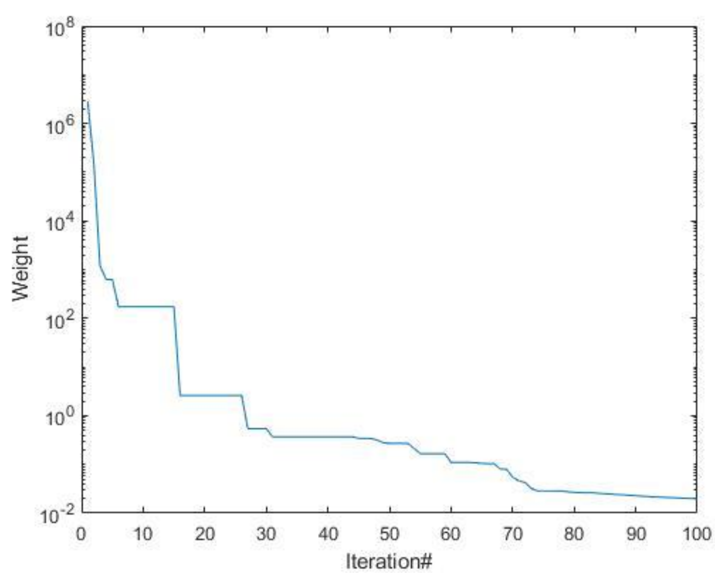

Figure 3.16 Convergence curve of PSO

As shown in figure 3.16, the fitness value improves over iterations providing insights into the optimization progress and convergence behavior of the PSO algorithm for tuning the PID controller in AGC. Generally, the flow chart of the particle swarm optimization was as shown below:

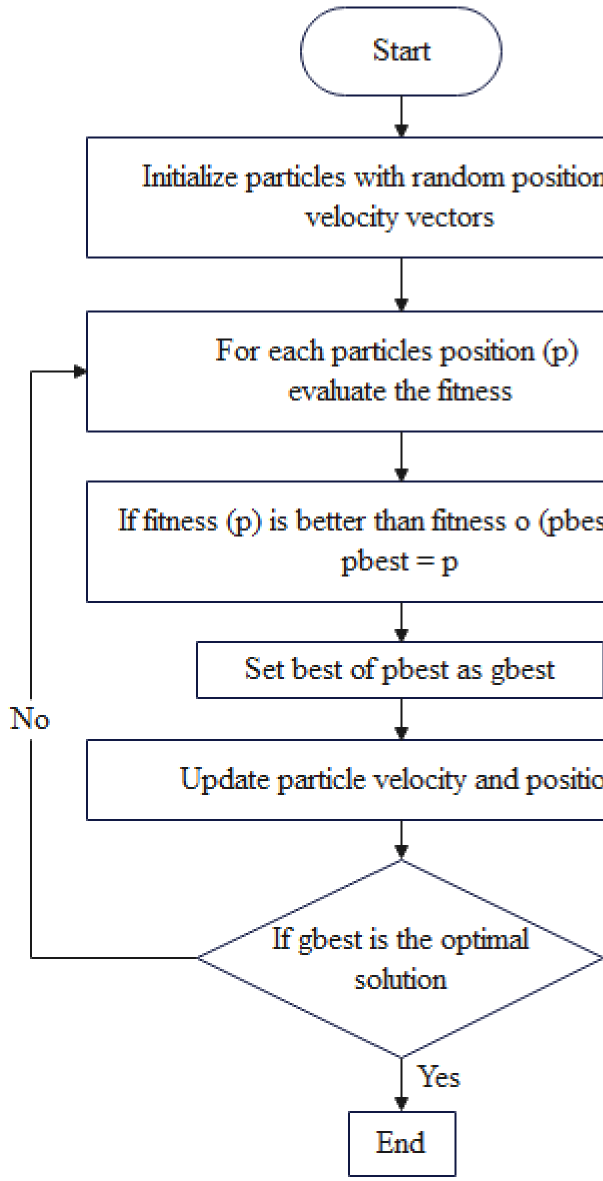

Figure 3.17 Flow chart of PSO

CHAPTER FOUR

RESULTS AND DISCUSSIONS

4.1 Introduction

This chapter delves into the simulation of interconnected power systems using Automatic Generation Control. It explores how the Particle Swarm Optimization technique can be used to find optimal settings for the controllers within the AGC system. Furthermore, the chapter examines the integration of renewable energy sources (photovoltaic and wind power) and energy storage systems (VRFB and FESS) into the power system, along with the implementation of various controllers and optimization techniques. The simulations were conducted using the MATLAB/Simulink software package, focusing on step responses. The mathematical models for all the AGC components were built using Simulink blocks, specifically designed for simulation purposes. This Simulink model serves as the foundation for running simulations and evaluating the performance of the controllers themselves, both with and without PSO optimization. Ultimately, the goal is to achieve the objectives outlined in the thesis through effective control strategies and optimization techniques.

4.2 Simulink Model of the proposed System

4.2.1 Simulink model of interconnected power system by AGC

Leveraging the governor, turbine, and power system equations derived in Chapter 3, we can construct a two-area AGC model. Figure 4.1 illustrates the Simulink model of this system, incorporating an integral controller.

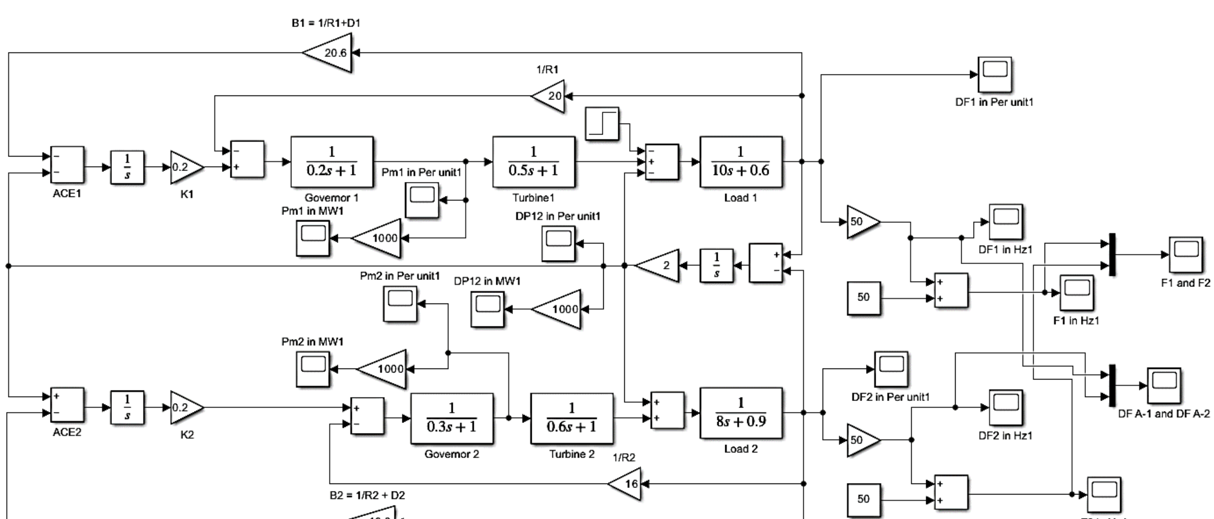

Figure 4.1 Simulink model of AGC of two area system without controller

The parameter values used in the Simulink model, some them are calculated as shown in the chapter three and the others are extracted from the above reviewed literatures in order to get better parameter values.

4.2.2 Simulink model of PV

This Simulink model of PV system have $1000W/m^2$ irradiance, 25 degrees Celsius temperature and produced a power output of 100 MW. The model represented the behavior of the solar panel in converting solar energy into electrical power, showcasing its efficiency and reliability under optimal operating conditions. The power measurement block in the model confirmed the output power level and demonstrating the capability of the PV system to generate a significant amount of power when exposed to optimal irradiance and temperature conditions.

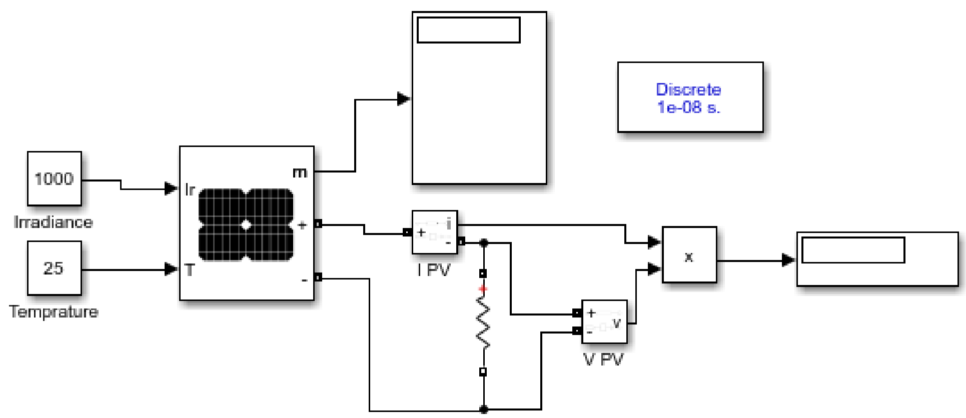

Figure 4.2 Simulink model of PV

The behavior of a PV system is highly dependent on the amount of irradiance it receives and temperature at which it operates. So, the efficiency and power output fluctuate throughout the day and across different seasons. When it comes to the AGC system PV was one of the renewable energy sources that can be used as an input to the power system in order to overcome the change occur in the areas and also the power in the power system. So, the PV cab be modelled by using first order transfer function as shown below in the AGC system. The parameter time constant used in this model was selected from reviewed literatures.

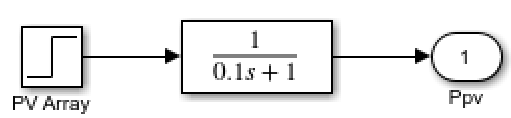

Figure 4.3 Simulink model of transfer function of PV

4.2.3 Simulink model of Wind

This Simulink model have a rated wind speed $11m/s$, a wind turbine radius of 38.2-meter with power output of 1.5 MW. Figure 4.4 shows the wind turbine model for the given output power. There are four inputs radius, wind speed, turbine rotor speed, lambda and beta, the output is power. Then the output power from this model was integrated to the power system controlled by AGC.

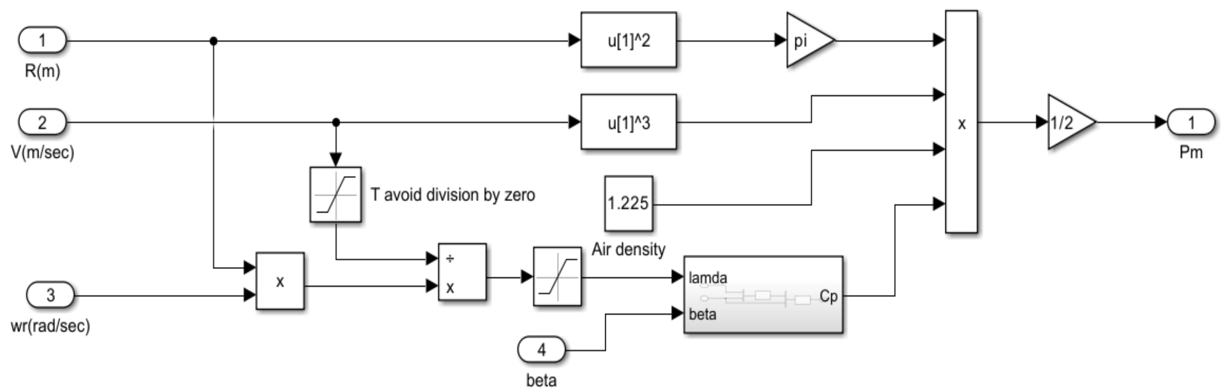

Figure 4.4 Simulink model of wind turbine

In the AGC system wind turbine can be represented by using first order transfer function as shown in figure below. The power output from the system can be used as an input to overcome the sudden power change occur in the areas and also supply power to the power system in order to increase the impact of renewable energy in power system.

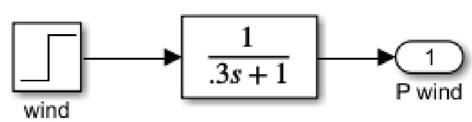

Figure 4.5 Simulink model of transfer function of wind turbine

4.2.4 Simulink model of Vanadium Redox Flow Battery

VRFB uses vanadium ions in various oxidation states to store chemical potential energy, which is then used during load perturbation. Because of the delayed response of the area control error and governor mechanism, an energy storage system can give additional energy support during a load disruption, therefore VRFB helping to stabilize the frequency deviation. The VRFB's analogous transfer function in terms of time constant has been applied to the charging and discharging notion. The Simulink linearized model of VRFB is as shown in figure 4.6. ACE signal of area-1 is used as the input for the VRFB system. The power reference is the rated power of battery connected which is 0.02pu. Parameters of time constants are extracted from the reviewed literatures. Then the output power from VRFB was integrated to the power system, depending on the input parameters of the model then the can store or supply power to the power system controlled by AGC.

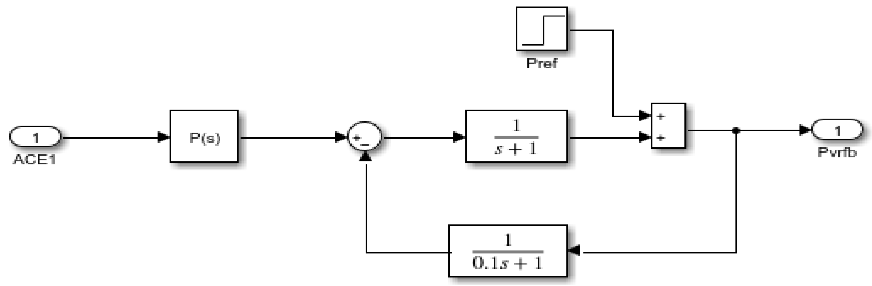

Figure 4.6 Simulink model of VRFB

4.2.5 Simulink model of FESS

The Simulink model of flywheel energy storage system is as shown in figure 4.7. The model represents the physical system that stores and releases energy in the form of kinetic energy stored in a rotating flywheel and have two parts the governing system and the flywheel model. This model has three inputs, area control error, reference electrical frequency and rotor speed of the flywheel. The parameter values used in the model are extracted from the specifications of the system released by the manufacturer company and parameters of time constants used in this model are selected from the reviewed literatures.

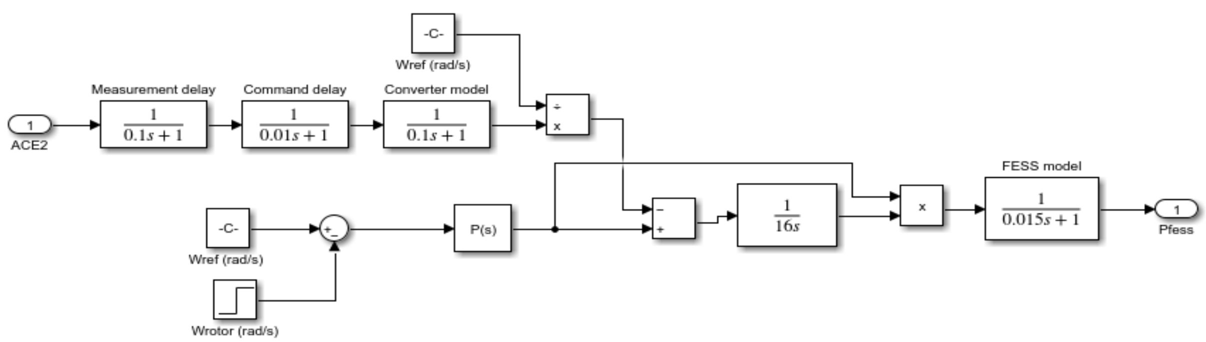

Figure 4.7 Simulink model of FESS

ACE represents the imbalance between generation and loads of each area, then the measurement delay receives and process based up on the measurement of the system parameters or ACE. After that command delay processing time for the control system to decide on the response then converter delay is a time needed to sending a control signal to flywheel energy storage system. So, if there is a frequency deviation due to imbalances of power then the control system adjusts the power flow either from or to the flywheel to stabilize the system. When power disturbance occurs in the power system the control system converts kinetic energy from the flywheel back in to electrical energy to control the power disturbance and frequency. A feedback signals from the ACE was used to adjust the power direction of the flywheel and ensuring the frequency deviation.

4.3 Simulation results of the system model with different controllers

The system model was modelled using the SIMULINK environment to simulate and analyze a load frequency and power control system and finding the optimal design of the controllers. The goal is to optimize controller design and minimize the objective function. To achieve this, a Particle Swarm Optimization (PSO) algorithm is incorporated into the model. The system's performance is evaluated under various conditions, including step load perturbation, integration of renewable energy integration and integration of energy storage systems. This evaluation validates the effectiveness of the proposed PSO approach. Different scenarios are investigated, including simulations with and without PSO to demonstrate its efficiency. The following scenarios are investigated.

4.3.1 Simulation results of two area AGC with integral controller

In this scenario, the two-area system was analyzed with and without integration of the chosen renewable energy sources and energy storage systems.

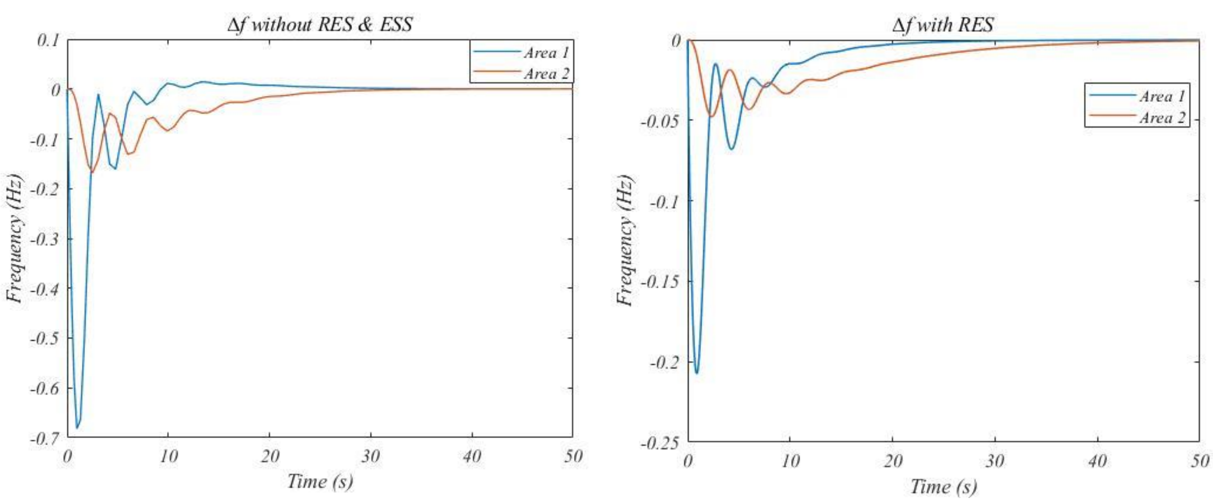

(a) (b)

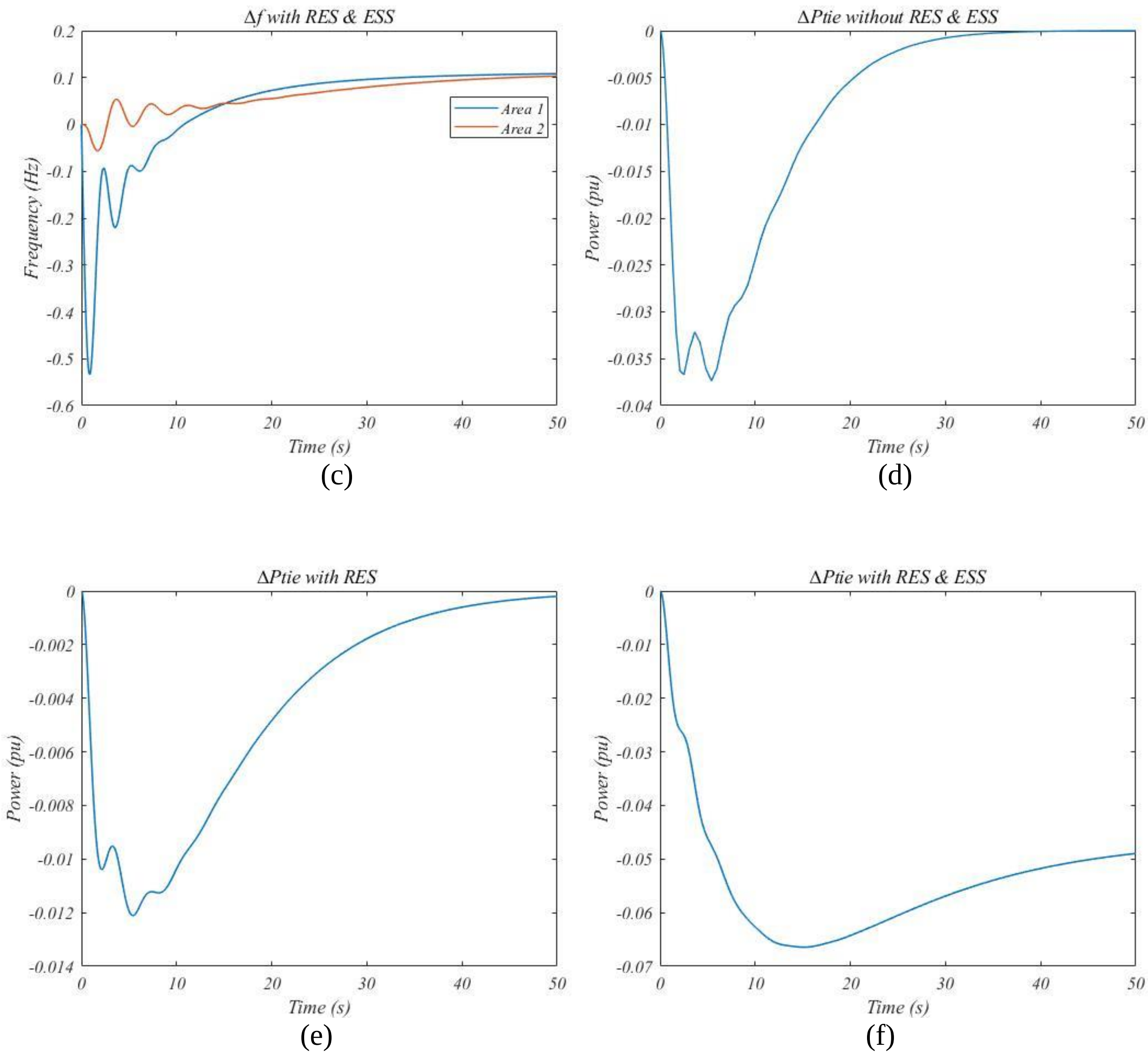

Figure 4.8 Δf *and* ΔP_{tie} *of: a & d without RES & ESS, b & e with RES, c & f with RES & ESS*

The goal of these scenarios was to evaluate the performance of the AGC system with integral controller when a step load disturbance of 0.2pu was occurred in the area-1 at t=0, as well as to see the performance when PV/wind/VRFB/FESS were integrated into the given system. The Simulink model for this scenario is illustrated in Figure 4.1. When a step load perturbation occurs in area-1, the frequency of both areas and tie line power deviates as indicated in figure 4.8. As we can see the system is on instability because of its high settling time in both areas and also high value of change in tie line power was occurred in the system which leads to the system instability. But the system needs better control strategies to minimize the change occur to get stability.

4.3.2 Simulation results of two area AGC with PID controller

In this case, the two area AGC system was examined by adding the PID controller on the system. Renewable energy sources and energy storage system are integrated to system in order to see the performance of the system when step load perturbation occurred. Here, PID controller was used in the Simulink model of the system as shown in figure 4.9.

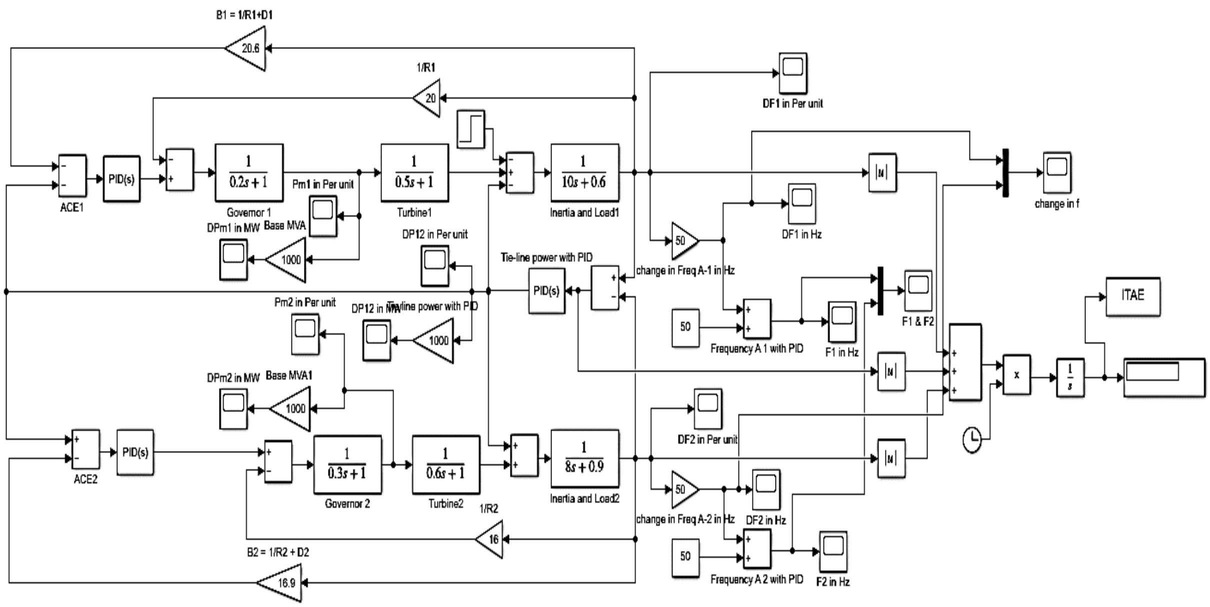

Figure 4.9 Simulink model of AGC of two area system with PID controller

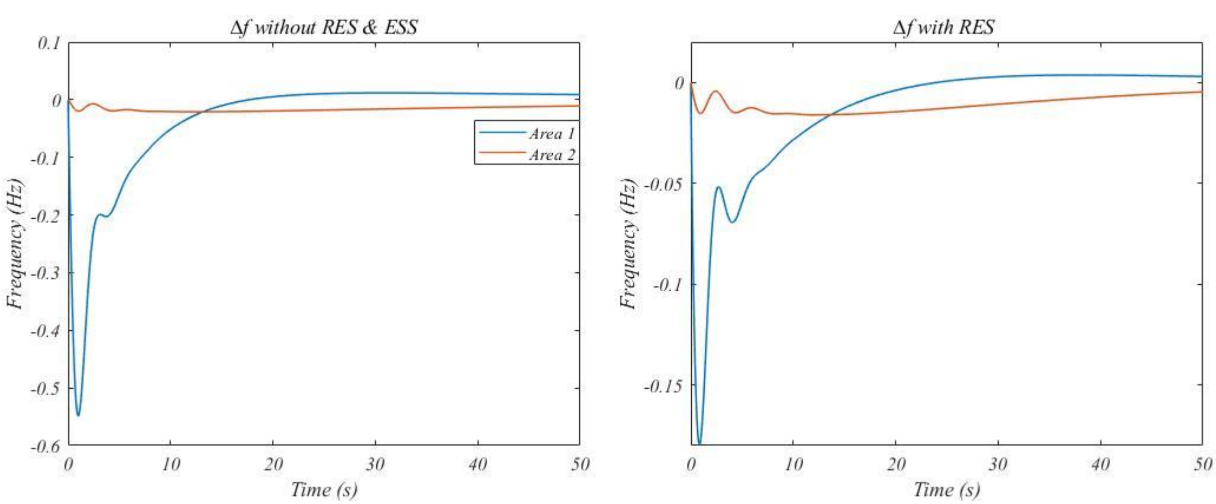

(a) (b)

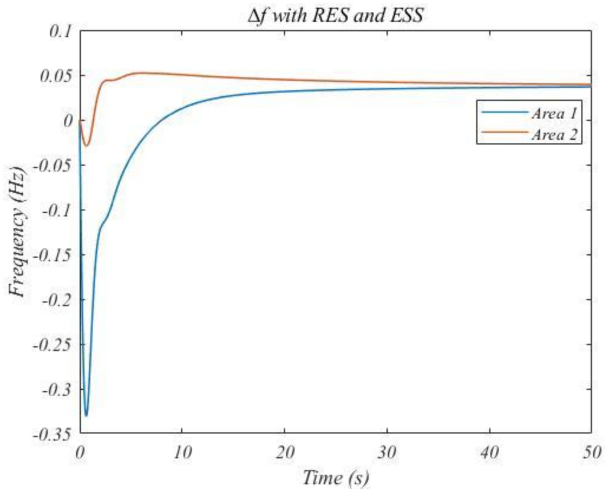

(c)

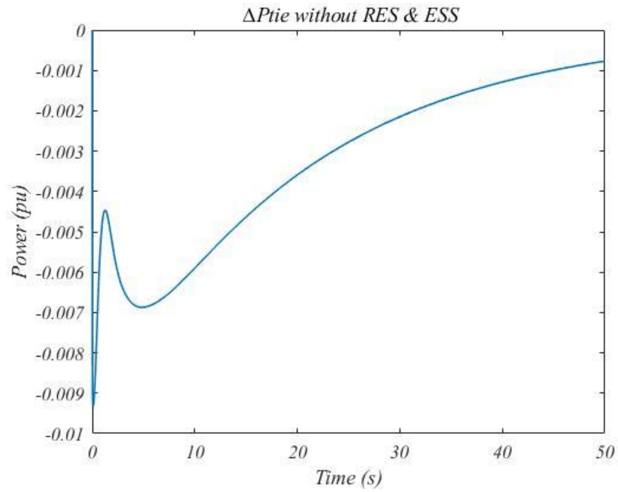

(d)

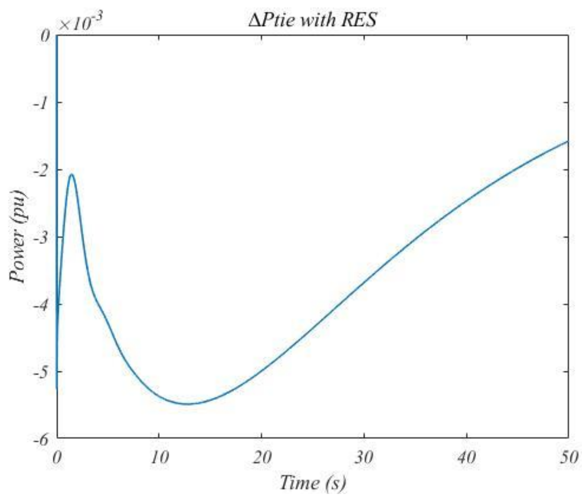

(e)

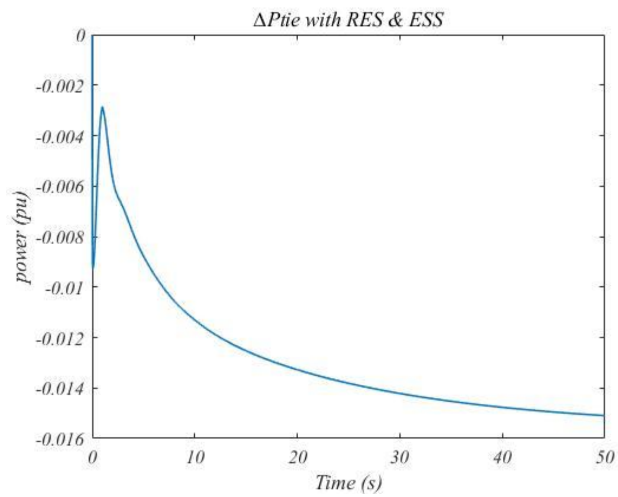

(f)

Figure 4.10 Δf and ΔP_{tie} of: a & d without RES & ESS, b & e with RES, c & f with RES & ESS

Figure 4.10 are shows the results of different scenarios depending on integration. When step load disturbance occurred in the above system then the dynamic response of change in frequency and change in tie line power are as shown in figure 4.10. As the result shows the frequency and tie line power deviations are somehow good when compared to the first scenarios but still it needs optimization because it has high settling time which causes the system to instability. The integration of renewable energy sources and energy storage system can support the system by improving the frequency and tie line power regulation when load perturbation occur. Somehow, they can regulate the power system frequency when they generate power and have stored energy in the power system.

4.3.3 Simulink results of PSO based AGC of the system without PV/wind/VRFB/FESS

In this case, the two area PSO based AGC system was examined by adding the PID controller on the system and PSO algorithm was used in order to optimize the gains of PID controllers. RES and ESS are included in power system model and PSO perform the optimization process. The primary goal of this scenario is to evaluate the performance of the proposed method PSO, which applies a step load disturbance of 0.2pu to area-1 at t = 0. Figures 4.11 shows the dynamic responses of the system including change in frequency at both area and change in tie line power respectively using the proposed PSO PID controller. The optimal gains of the PID controllers by using PSO algorithm are as shown in Table 4.1. As we can see the system response using PSO based PID controller have lower area steady state error and better frequency and tie line regulation than the PID controller without the optimization algorithm. So, the PSO algorithm have shown better performance in minimizing the settling time of the change in frequency and change in tie line power.

Table 4.1 Optimal values of the PSO based PID controller

PID	K_p	K_i	K_d
1	1	0.3372	0.9987
2	1	-0.0046	-2.8852e-06
3	0.8127	0.8097	-0.6738

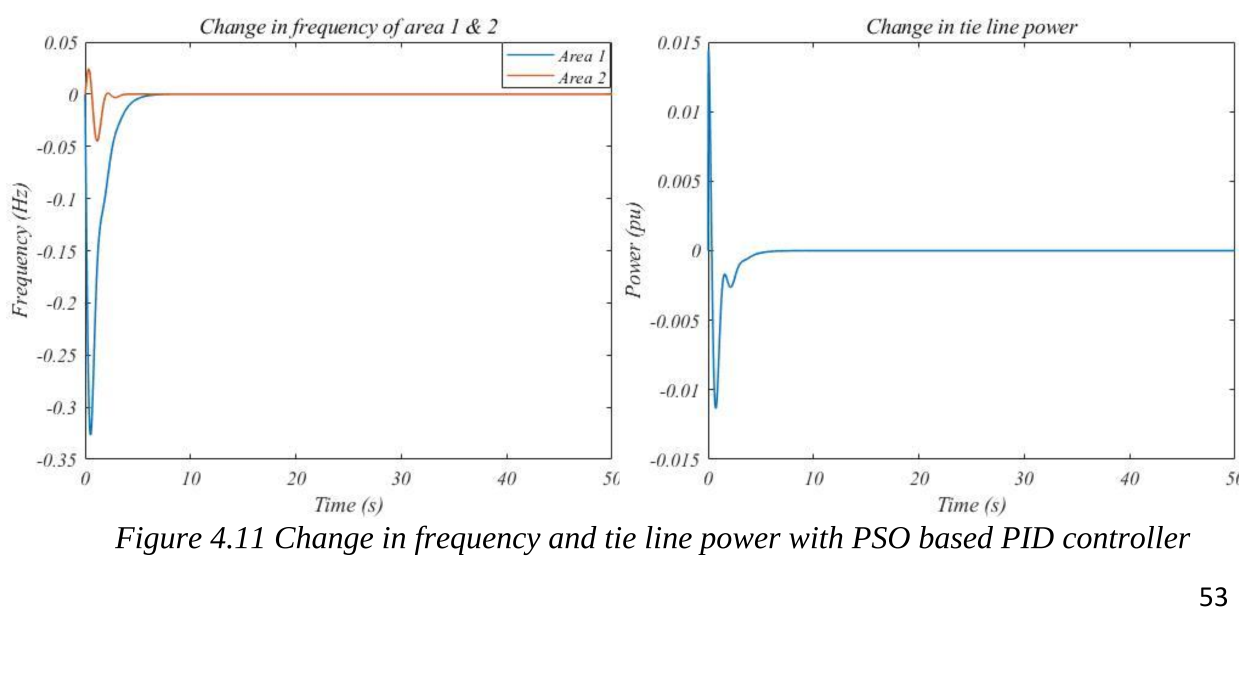

Figure 4.11 Change in frequency and tie line power with PSO based PID controller

4.3.4 Simulink results of PSO based AGC of two area with PV/wind integration

In this scenario, the power system performance was evaluated by integrating renewable energy sources which is PV and wind into the system as shown in figure 4.12. The rated output power extracted from the PV power plants was used which is $0.1\ pu$. The output power used was when the rated value of wind speed occurred which is $0.051\ pu$**.** The PID controllers are optimally designed by using PSO algorithm with optimal values as shown in table 4.2. These values are gained by using PSO algorithm technique after 100 iterations in the simulation model and the minimum objective function value after 100 iteration is 0.02359. The simulation outcomes shown in figure 4.13, shows the robustness of the proposed controllers to deal with the integration of PV and wind uncertainty and load variability. The settling time of the frequency of both areas decreased from 23.12s to 4.74s and 48.96s to 5.73s for area 1 and 2 respectively.

Table 4.2 Optimal values of the PSO based PID with RES

PID	K_p	K_i	K_d
1	0.4857	0.8232	0.2981
2	0.8514	1	0.7627
3	1	-3.0797e-06	1

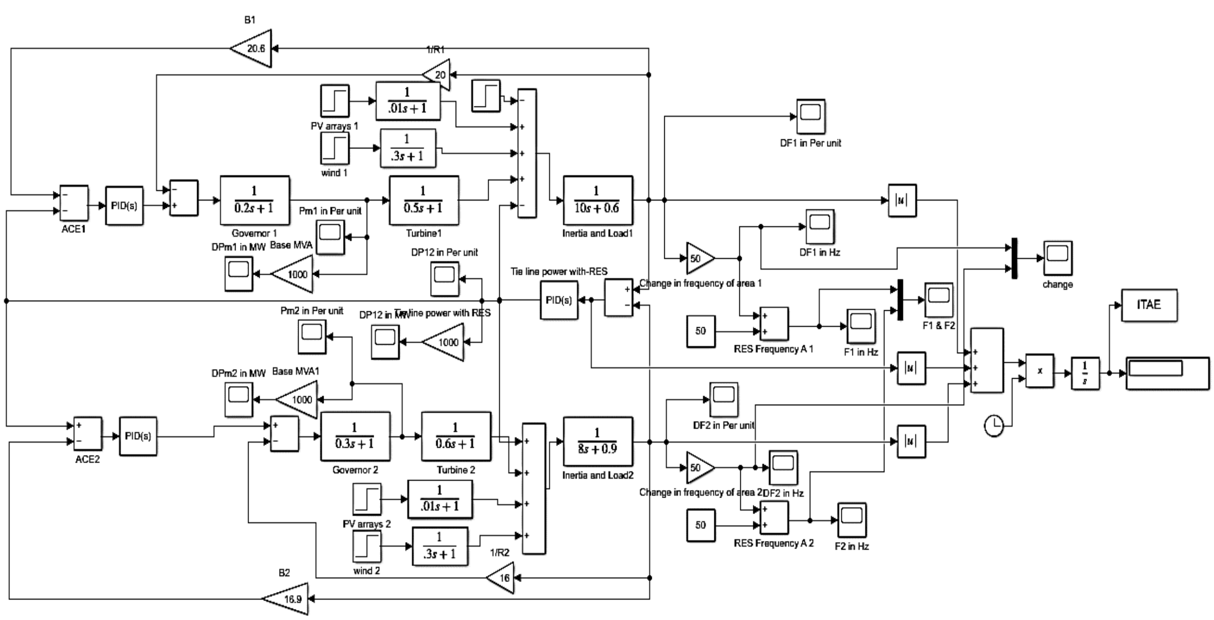

Figure 4.12 Simulink model of AGC of two area system with integration of PV & wind

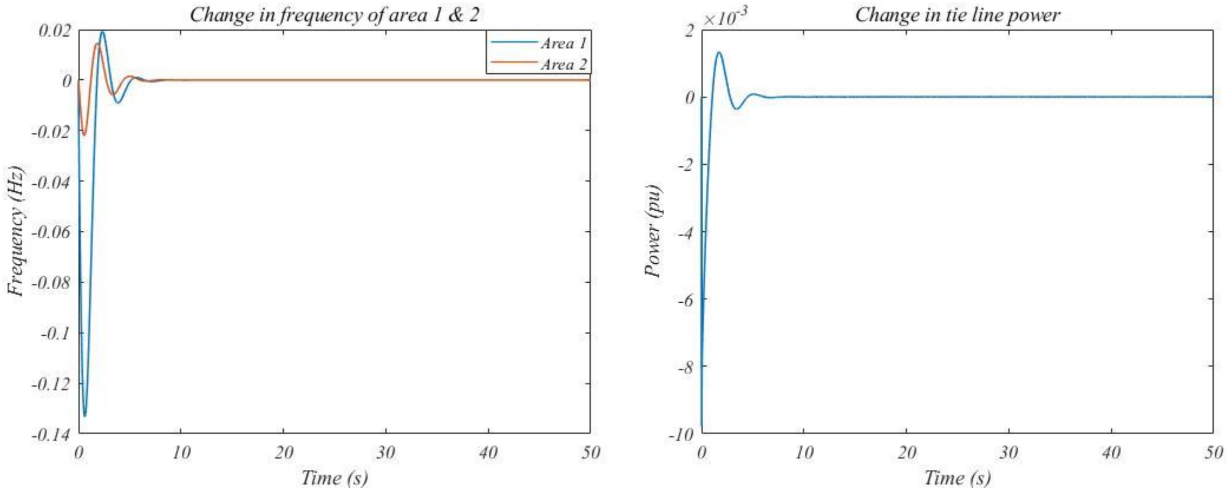

Figure 4.13 Change in frequency and tie line power of PSO based PID with integration of PV & wind

4.3.5 Simulink results of PSO based AGC of two area with PV/wind/VRFB/FESS

In this case, the impacts of penetrations of RES and ESS in to the power system model are analyzed. Two ESS are used in this scenario, FESS and VRFB was integrated to the simulated model as revealed in figure 4.14. PSO based PID controllers are used in order to optimize optimal value for the controllers, the optimal values of PSO based PID controllers that included RES and ESS are as revealed in table 4.3. The PSO method obtains a minimum objective function value of 0.019889. The Simulink model power system when PV/wind/VRFB/FESS integrated to the AGC system model are as shown in figure below. The results show that change in frequency and tie line power deviations are significantly reduced. The settling time of the change in frequency was decreased from 16.9 to 4.12 and 3.01 to 9.68 for both area 1 and 2 respectively.

Table 4.3 Optimal values of the PSO based PID with PV/wind/VRFB/FESS

PID	K_p	K_i	K_d
1	0.3233	1	0.3933
2	0.0277	0.1903	0.2157
3	0.4902	8.8210e-05	-0.0209

This values of PID controller are the optimal value of PID gains which determined by the PSO algorithm technique. At this optimal point the system was controlled the power perturbation occurred and integration of PV/wind/VRFB/FESS in to the power system model with high performance in order to maintain the stability and reliability of the power system.

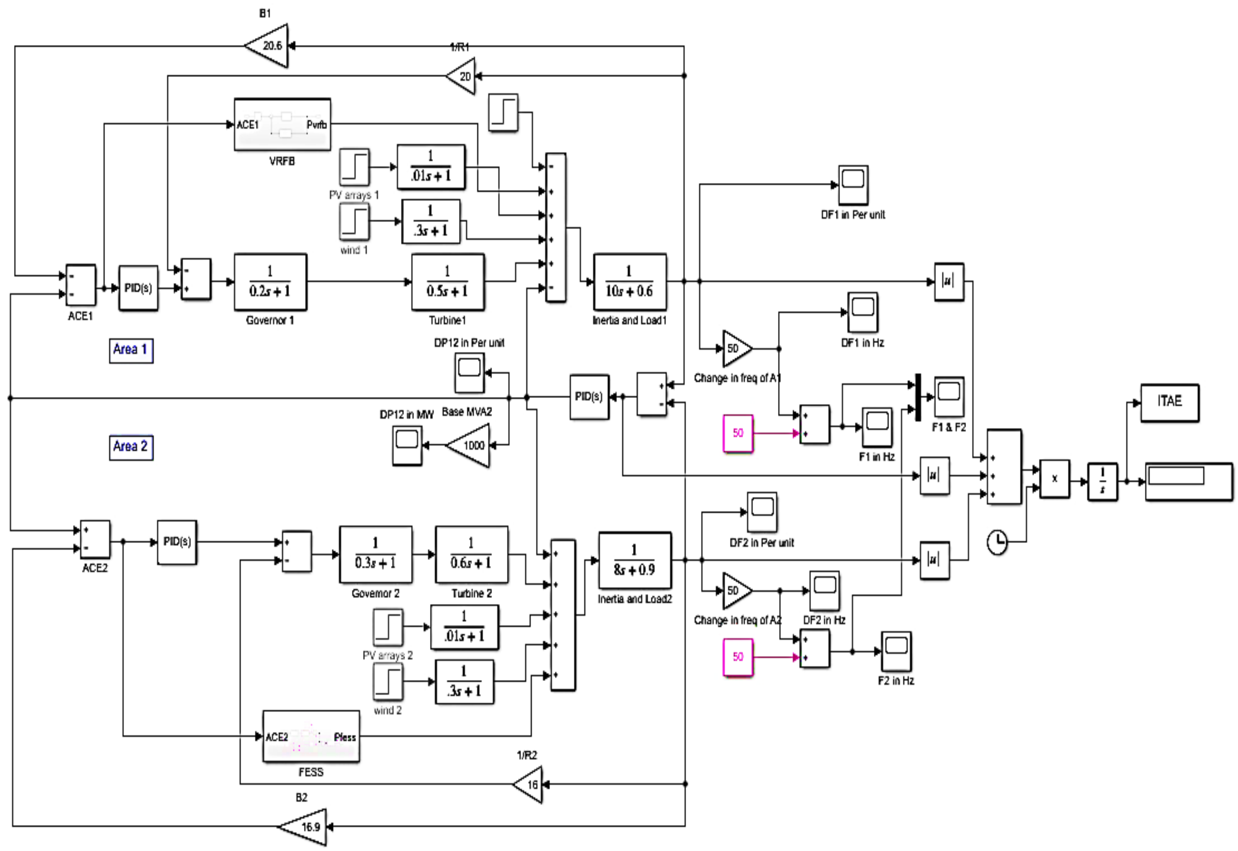

Figure 4.14 Simulink model of AGC of two area system with integration of PV/wind/VRFB/FESS

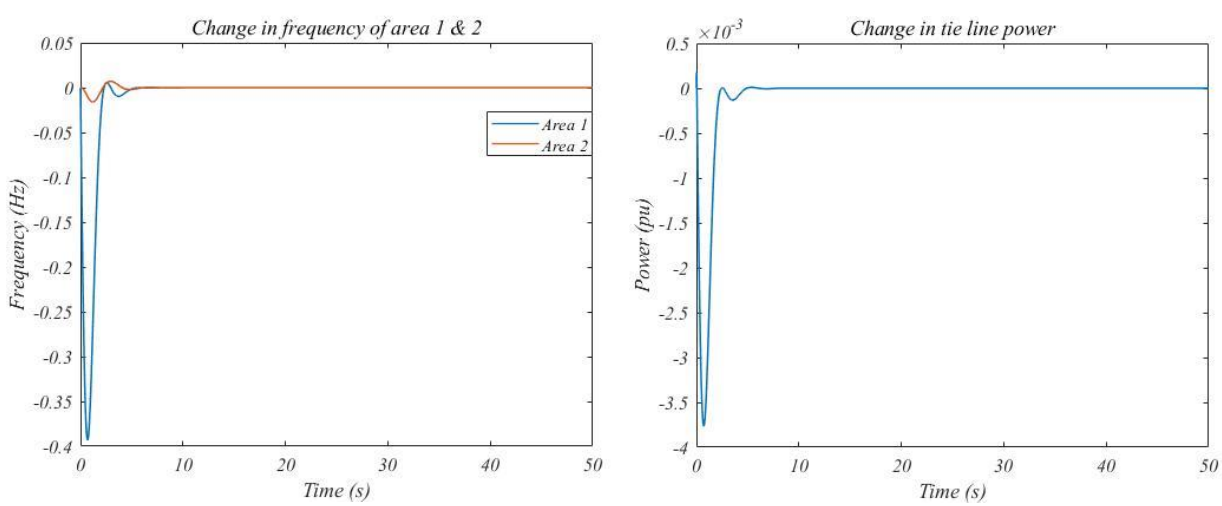

Figure 4.15 Change in frequency and tie line power PSO based PID with integration of PV/wind/VRFB/FESS

4.4 Comparisons of the Simulink results

PSO based PID controller was improved the change in both time domain and frequency domain which leads to the frequency of system to the nominal frequency. Moreover, when PV/wind/FESS/VRFB integrated into the power system the change in frequency and tie line power was decreased. The settling time for the frequency area-1 was decreased from 15.032s to 4.7416s and 35.9944s to 9.6857s in area-2. Finally, figure 4.16, 4.17 and 4.18 shows comparisons of the frequency and tie line power. The integration of RES and ESS to the power system was controlled by the proposed algorithm and the change in frequency occur and also tie line power shows better performance than other.

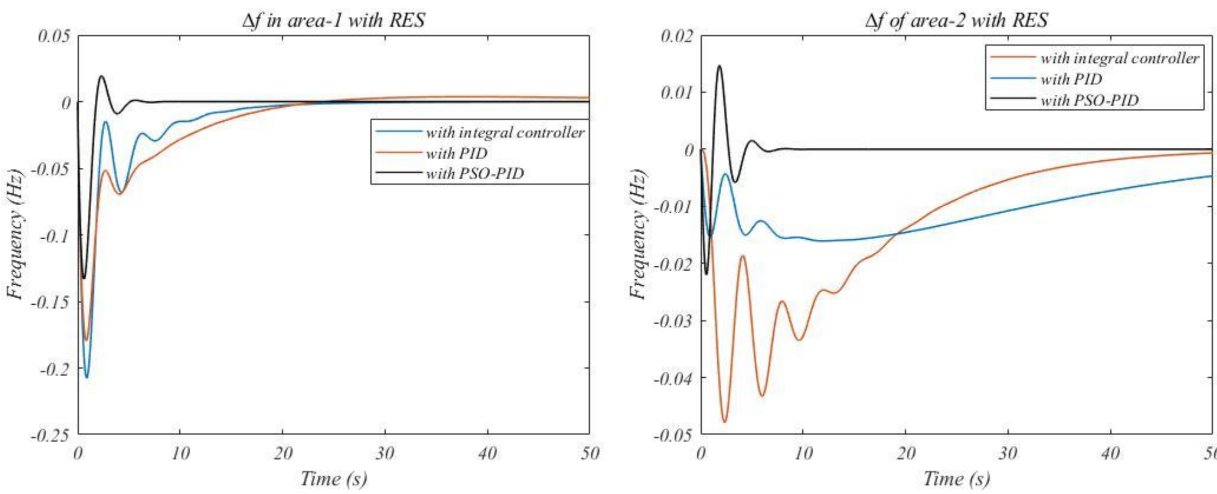

Figure 4.16 Comparisons of change in frequency in area 1 & 2 with RES integration

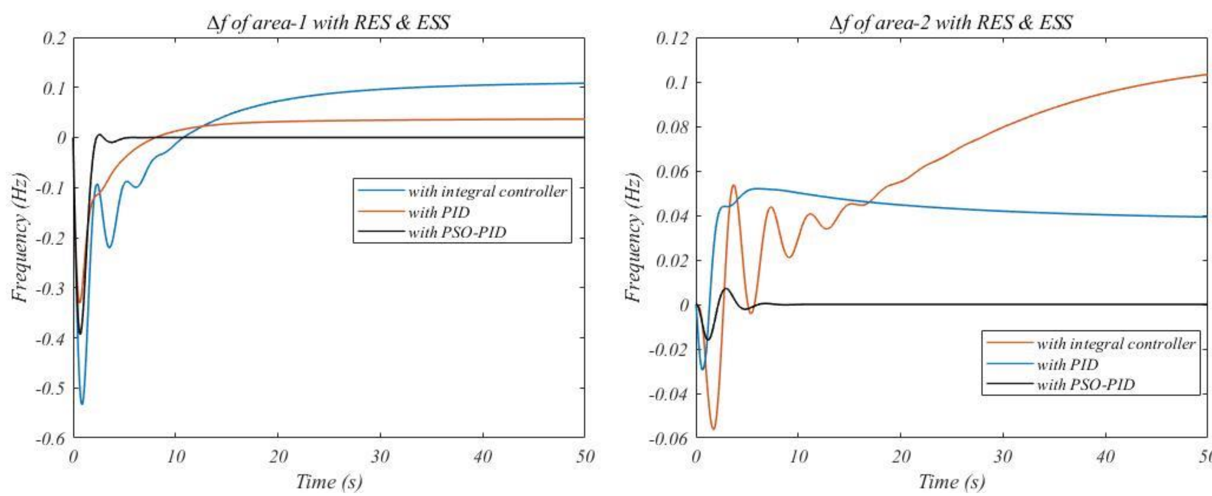

Figure 4.17 Comparisons of change in frequency in area-1 & 2 with RES and ESS integration

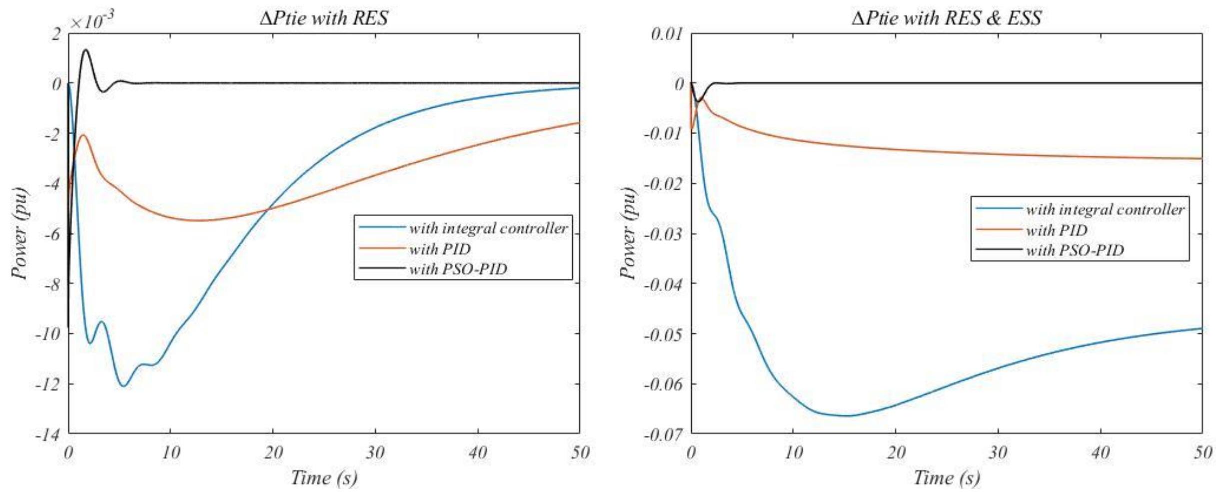

Figure 4.18 Comparisons of change in tie line power with RES and ESS integration

As the result shows the proposed control system has shown better performance in controlling the load perturbation and integration of PV/wind/VRFB/FESS into power system. The change in frequency and tie line power are regulated effectively with minimum settling time which leads to ensuring the reliability and stability of the power system. Therefore, using PSO based AGC system for controlling the integration of renewable energy sources and energy storage systems are best solutions and also enhance the integration of renewable energy sources into power systems.

CHAPTER FIVE

CONCLUSION AND RECOMMENDATION

5.1 Conclusion

In this thesis, an interconnected power system model has been presented and simulated within AGC system. Integration of PV/wind from renewable energy and VRFB/FESS from energy storage system to the system model was included with the detailed modelling of RES and ESS components such as wind, PV, VRFB and FESS. For the purpose of establishing a realistic system model, different real data are injected to the simulation model. This thesis also proposed PSO algorithm to optimally tuned the PID controllers under different scenarios. The study attempts to improve the performance of AGC under SLP and renewable energy sources uncertainty by ensuring optimal PSO based PID control and integration of ESS. Different scenarios were individually simulated to evaluate the proposed PSO based AGC incorporating hybrid wind/PV/VRFB/FESS. Simulation was carried out by using MATLAB/SIMULINK. The simulation results have proven that the proposed work performed more effectively with lower frequency and tie line power deviations, minimum steady state error and better damped under different operating conditions such as RES uncertainty and load variability. The settling time when the proposed algorithm used shows an excellent performance in dealing with the RES and ESS penetration by optimizing the controller. Finally, in order to enhance renewable energy integration to the power system such proposed system was needed to overcome related problems like stability, reliability and uncertainty of renewable energy.

5.1 Future Works

As observed in the simulation two area AGC system was used but it is better to use multi area system in order to control vast area of power system. There are different types of renewable energy sources in the world, so they should have to integrated to the power system by using proper controlling strategy. Since energy storage systems are crucial for renewable energy resources to help address the intermittent nature of renewable energy generation and to ensure a stable and reliable energy supply, hence using recent storage system like Tesla Megapack energy storage and Hydrogen based energy storage provides power system stabilization, peak shaving, very high energy density, high storage capacity and so on. Also, to make the controller more advanced, it’s better to include an artificial neural network (ANN) and machine learning algorithms because they are recent technologies used to enhance the performance and adaptability of control strategies in power systems ultimately contributing to the stability and reliability of the system.

REFERENCES

Abazari, A., & Monsef, H. (2019). Coordination Strategies of Distributed Energy Resources including FESS , DEG , FC and WTG in Load Frequency Control (LFC) Scheme of Hybrid Isolated Micro-grid. *International Journal of Electrical Power & Energy Systems*, *109*, 535–547. https://doi.org/10.1016/j.ijepes.2019.02.029

Amiryar, M. E., & Pullen, K. R. (2020). Analysis of standby losses and charging cycles in flywheel energy storage systems. *Energies*, *13*(17). https://doi.org/10.3390/en13174441

Ang, K.H., Chong, G. and Li, Y. (2007). PID Control System Analysis , Design , and Technology. *IEEE Transactions on Control Systems Technology*, *13*(4), 559–576.

Castillo, A., & Gayme, D. F. (2014). Grid-scale energy storage applications in renewable energy integration : A survey. *ENERGY CONVERSION AND MANAGEMENT*, *87*, 885–894. https://doi.org/10.1016/j.enconman.2014.07.063

Dassisti, M., Mastrorilli, P., & Cozzolino, G. (2021). Vanadium : A Transition Metal for Sustainable Energy Storing in Redox Flow Batteries. *Encyclopedia of Smart Materials*, 208–229. https://doi.org/10.1016/B978-0-12-803581-8.04007-8

Dhawane, V., & Bichkar, R. (2020). AUTOMATIC GENERATION CONTROL OF A THERMAL POWER PLANT WITH REHEAT TURBINE USING PSO OPTIMIZED INTEGRAL. *International Journal of Electrical Engineering and Technology*, *11*(4), 318–330.

Dr. Ajay Mathur. (2023). *World Solar Market Report 2023*.

Ghoshal, S. P. (2004). Optimizations of PID gains by particle swarm optimizations in fuzzy based automatic generation control. *Electric Power Systems Research*, *72*(3), 203–212. https://doi.org/10.1016/j.epsr.2004.04.004

Gozde, H., & Taplamacioglu, M. C. (2011). Automatic generation control application with craziness based particle swarm optimization in a thermal power system. *International Journal of Electrical Power and Energy Systems*, *33*(1), 8–16. https://doi.org/10.1016/j.ijepes.2010.08.010

GWEC. (2023). *GWEC | GLOBAL WIND REPORT 2023*.

Hasanien, H. M. (2017). Whale optimisation algorithm for automatic generation control of interconnected modern power systems including renewable energy sources. *The Institution of Engineering and Technology*, *12*(3), 607–614. https://doi.org/10.1049/iet-gtd.2017.1005

Kebede, A. A., Mekonen, T., Ayele, H., & Ramu, G. (2016). Performance Analysis of Power Quality Impact of Adama-One Wind Farm in Ethiopia. *In 2016 International Confernce on Control, Instrumentation, Communication and Computational Technologies (ICCICCT)*, 813–819.

Kumar, A., & Shankar, R. (2021). A Quasi Opposition Lion Optimization Algorithm for Deregulated AGC Considering Hybrid Energy Storage System. *Journal of Electrical Engineering & Technology*, *16*(6), 2995–3015. https://doi.org/10.1007/s42835-021-00835-0

Li, J., Sun, Y., & Hou, S. (2021). Particle Swarm Optimization Algorithm with Multiple Phases for Solving Continuous Optimization Problems. *Discrete Dynamics in Nature and Society*, *2021*.

Lourenssen, K., Williams, J., Ahmadpour, F., Clemmer, R., & Tasnim, S. (2019). Vanadium redox fl ow batteries : A comprehensive review. *Journal of Energy Storage*, *25*, 100844. https://doi.org/10.1016/j.est.2019.100844

Martínez, M., Molina, M. G., & Mercado, P. E. (2017). Optimal sizing method of vanadium redox flow battery to provide load frequency control in power systems with intermittent renewable generation. *IET Renewable Power Generation*, *11*(14), 1804–1811. https://doi.org/10.1049/iet-rpg.2016.0798

Martins, H. (2023). Integration of Renewable Energy Sources in Power Systems : Challenges and Solutions. *Journal of Electrical & Electronic Systems*, *12*, 1–2. https://doi.org/10.37421/2332-0796.2023.12.42

Merei, G., Magnor, D., Leuthold, M., & Sauer, D. U. (2014). Optimization of an Off-grid Hybrid Power Supply System Based on Battery Aging Models for Different Battery Technologies. *IEEE 36th International Telecommunications Energy Conference(INTELEC)*, 1–6.

Palanisamy, K., & Padmanaban, S. (2018). Intelligence-Based Battery Management and Economic Analysis of an Optimized Dual-Vanadium Redox Battery for a Wind-PV Hybrid System. *Energies*, *11*(10), 2785. https://doi.org/10.3390/en11102785

Panda, S., Mohanty, B., & Hota, P. K. (2013). Hybrid BFOA-PSO algorithm for automatic generation control of linear and nonlinear interconnected power systems. *Applied Soft Computing Journal*, *13*(12), 4718–4730. https://doi.org/10.1016/j.asoc.2013.07.021

Power, E. E. (2019). *METEHARA SOLAR POWER PV PLANT ENVIRONMENTAL AND SOCIAL IMPACT ASSESSMENT VOLUME 1 : MAIN REPORT* (Vol. 1).

Puleston, T., Clemente, A., & Costa-castelló, R. (2022). Modelling and Estimation of Vanadium Redox Flow Batteries : A Review. *Batteries*, *8*(9), 121.

Qin, R., Chen, J., Li, Z., Teng, W., & Liu, Y. (2023). Simulation of Secondary Frequency Modulation Process of Wind Power with Auxiliary of Flywheel Energy Storage. *Sustainability (Switzerland)*, *15*(15). https://doi.org/10.3390/su151511832

Sambariya, D. K., & Fagana, R. (2017). Load Frequency Control of Multi-Area Hydro Thermal Power System Using Elephant Herding Optimization Technique. *Journal of Automation and Control*, *5*(1), 25–36. https://doi.org/10.12691/automation-5-1-5

Shaikh, M., & Yadav, D. (2022). A REVIEW OF PARTICLE SWARM OPTIMIZATION (PSO) ALGORITHM. *International Journal of Mechanical Engineering and Technology (IJMET)*, *13*(7), 19–44.

Suvire, G. O., Ontiveros, L. J., & Mercado, P. E. (2017). Combined control of a flywheel energy storage system and a vanadium redox flow battery for wind energy applications in microgrids. *Dyna*, *84*(202), 230–238.

Talukder, S. (2011). *Mathematical Modelling and Applications of Particle Swarm Optimization*.

Tasnin, W., & Saikia, L. C. (2018). Comparative performance of different energy storage devices in AGC of multi-source system including geothermal power plant. *Journal of Renewable and Sustainable Energy*, *10*(2). https://doi.org/10.1063/1.5016596

Xu, K., Guo, Y., Lei, G., & Zhu, J. (2023). A Review of Flywheel Energy Storage System Technologies. *Energies*, *16*(18), 6462.

APPENDIX

Appendix-1

1. Characteristics of Metehara PV power plant (Power, 2019)

Parameter	Value
Power	100MW
Irradiation	1000W/m^2
Temperature	25ºC
Air Mass	1.5
DC output under STC	100Wp-350Wp

2. Wind turbine data of Adama I wind farm

Parameter	Value
Wind turbine nominal power	1.5 MW
Number of turbines	34
Inertia constant	4.32
Rated wind speed	11 m/s
Cut in wind speed	3 m/s
Cut out wind speed	22 m/s
Rotor diameter	77
Optimal speed ratio	6.14
Maximum power coefficient	0.5
Swept area	4656 m^2
Number of blades	3
Air density	1.225 kg/m^3

3. Data of performance parameters of INVINITY VS3-022 VRFB specifications

Item	Value
Operating voltage range	750 - 950 VDC
Energy storage capacity	230 kWh
Max. DC current	104 A
Max. DC power	78 kW
Depth of discharge	0 – 100%
Overcurrent protection device	Integrated
Continuous discharge	8 h @ 29 KW 4 h @ 52 KW 2.25 h @ 75 KW
Design life	> 25 years
Cycle life	> 20,000 cycles
Lifetime throughput	> 4,000 MWh
Response time	> 200 milliseconds
Operating temperature	-5ºC to 45ºC
Cooling	Forced air
Operating humidity	0 to 95% RH

4. Data of Parameters of FESS specifications

Parameter	Value
Energy Capacity per flywheel	100 kW
Energy delivery per flywheel	25 kWh
Discharge time at rated capacity	15 minutes
Cycle life	100,000 cycles
Design life	> 20 years
Input / output voltage	480 VAC
Frequency	50 Hz or 60 Hz
Standby loss	0.03 MWh
Round trip efficiency	85%
Response time	< 1 second to full power
Operating rotational speed	8,000 – 16,000 rpm
Moment of inertia	32 $kg.m^2$
Number of poles	4
Flywheel Motor / Generator	Permanent magnet synchronous
Temperature range	-35ºC to +40ºC
Humidity	Up to 95%

Appendix-2

MATLAB code of particle swarm optimization

```
% PSO for PID tuning

% Problem details

nVar = 9;

ub = [1 1 1 1 1 1 1 1 1];

lb = [-1 -1 -1 -1 -1 -1 -1 -1 -1];

fobj = @tunning;

% PSO parameters

noP = 15;

maxIter = 100;

wMax = 1;

wMin = 0.1;

c1 = 2;

c2 = 2;

vMax = 0.2 * (ub – lb);

vMin = -vMax;

% Initialize particles

For k = 1:noP

  Swarm.Particles(k).X = rand(1, nVar) .* (ub – lb) + lb;

  Swarm.Particles(k).V = zeros(1, nVar);

  Swarm.Particles(k).PBEST.X = zeros(1, nVar);

  Swarm.Particles(k).PBEST.O = inf;
```

```
  Swarm.GBEST.X = zeros(1, nVar);

  Swarm.GBEST.O = inf;

End

% Main loop

For t = 1:maxIter

  % Calculate objective values

  For k = 1:noP

    currentX = Swarm.Particles(k).X;

    Swarm.Particles(k).O = fobj(currentX);

    % Update PBEST

    If Swarm.Particles(k).O < Swarm.Particles(k).PBEST.O

      Swarm.Particles(k).PBEST.X = currentX;

      Swarm.Particles(k).PBEST.O = Swarm.Particles(k).O;

    End

    % Update GBEST

    If Swarm.Particles(k).O < Swarm.GBEST.O

      Swarm.GBEST.X = currentX;

      Swarm.GBEST.O = Swarm.Particles(k).O;

    End

  End

  % Update velocity and position

  W = wMax – t * (wMax – wMin) / maxIter;

  For k = 1:noP
```

```
Swarm.Particles(k). V = w.* Swarm.Particles(k). V + c1. * rand (1, nVar). *
        (Swarm.Particles(k). PBEST.X -Swarm.Particles(k).X)
    + c2. * rand(1,nVar) .* (Swarm.GBEST.X - Swarm.Particles(k).X);
  % Check velocities
  Swarm.Particles(k).V = max(min(Swarm.Particles(k).V, vMax), vMin);
  Swarm.Particles(k).X = Swarm.Particles(k).X + Swarm.Particles(k).V;
  % Check positions
  Swarm.Particles(k).X = max(min(Swarm.Particles(k).X, ub), lb);
 End
 % Display results
 Disp([‘Iteration# ‘, num2str(t), ‘ Swarm.GBEST.O = ‘, num2str(Swarm.GBEST.O)]);
 cgCurve(t) = Swarm.GBEST.O;
end
semilogy(cgCurve);
xlabel(‘Iteration#’);
ylabel(‘Weight’);
```